



OPEN

## Seasonal groundwater quality analysis in a drought prone agricultural region using GIS and IWQI for nitrate contamination insights

Abdessalam Laoufi<sup>1</sup>, Sabrine Guettaia<sup>1</sup>, Abderezak Boudjema<sup>1</sup>, Abdessamed Derdour<sup>2,3</sup>, Abdulrahman Seraj Almalki<sup>4</sup>, Amanuel Kumsa Bojer<sup>5</sup>✉, Khaled A. El-Nagdy<sup>6</sup> & Enas Ali<sup>7</sup>

The Hennaya Plain's groundwater resources, which are crucial for agricultural irrigation, face significant quality challenges driven by human-induced environmental transformations. This study comprehensively evaluated groundwater quality during both dry and wet seasons. The assessment used an integrated approach that synergistically combined the Irrigation Water Quality Index (IWQI) with high-resolution nitrate content analysis as complementary diagnostic tools. This combined methodology enabled a detailed evaluation of seasonal groundwater dynamics. Thirty-nine groundwater samples were collected from wells distributed across the plain. The research systematically evaluated physicochemical parameters and their seasonal variations. The investigation revealed contrasting seasonal patterns in groundwater quality parameters.  $\text{NO}_3^-$ -N contamination increased markedly from the dry to wet season, with the percentage of samples exceeding permissible levels rising from 12.82 to 69.23%. Conversely, chloride contamination decreased during the wet season, with exceedances dropping from 23.07 to 10.26% of samples. IWQI analysis indicated a marginal improvement in overall water quality during the wet season, which contrasted with a simultaneous escalation in nitrate pollution from moderate to severe levels. The integrated assessment categorized irrigation water quality as moderate to poor, highlighting the intricate interactions between agricultural practices, seasonal precipitation, and groundwater chemistry. These findings underscore the urgent need for comprehensive groundwater management strategies that address seasonal variability and anthropogenic influences on water resources.

**Keywords** Hennaya plain, Groundwater quality, Irrigation water quality index, nitrate pollution

Globally, groundwater serves as a fundamental lifeline for agricultural, industrial, and domestic water requirements, constituting approximately 97% of the planet's freshwater resources<sup>1,2</sup>. However, these vital systems face unprecedented threats from escalating anthropogenic pressures, climate change impacts, and unsustainable resource management strategies<sup>3,4</sup>. Groundwater contamination in semi-arid agricultural regions represents one of the most pressing water security challenges of the 21st century, with nitrate pollution being particularly prevalent in intensive agricultural areas worldwide<sup>5-7</sup>. Several large aquifers in arid and semi-arid areas have experienced severe nitrate pollution due to the impacts of intense agriculture, for example in the

<sup>1</sup>Laboratory n°25 Promotion of Water, Mineral and Soil Resources. Environmental Legislation and Technological Choices, University of Tlemcen, PO Box 119, Tlemcen 13000, Algeria. <sup>2</sup>Artificial Intelligence Laboratory for Mechanical and Civil Structures, and Soil, University Center of Naama, P.O. Box 66, Naama 45000, Algeria.

<sup>3</sup>Laboratory for the Sustainable Management of Natural Resources in Arid and Semi-arid Zones, University Center of Naama, P.O. Box 66, Naama 45000, Algeria. <sup>4</sup>Civil and Environmental Engineering Department, College of Engineering and Computing in Al-Qunfudhah, Umm Al-Qura University, Mecca, Saudi Arabia. <sup>5</sup>Ethiopian Artificial Intelligence Institute, PO Box 40782, Addis Ababa, Ethiopia. <sup>6</sup>Department of Civil Engineering, College of Engineering, Taif University, P.O. BOX 11099, Taif 21944, Saudi Arabia. <sup>7</sup>Faculty of Engineering and Technology, Future University in Egypt, New Cairo 11835, Egypt. ✉email: amanuel.kumsa@aau.edu.et

northern Mexico, southwest United States, India, and the North China Plain<sup>8–12</sup>, illustrating the consequences of poor groundwater management.

The global groundwater landscape exhibits significant spatial and temporal heterogeneity, with contamination risks intensifying across diverse regions. Recent comprehensive assessments reveal the alarming state of global groundwater systems, with approximately 50% experiencing significant degradation<sup>8,9</sup>. Agricultural practices contribute to over 70% of groundwater contamination in developing regions, primarily through intensive fertilizer application, irrigation return flows, and inadequate waste management<sup>10–17</sup>. In India's Punjab region, for instance, decades of agricultural intensification have resulted in groundwater nitrate levels exceeding 100 mg/L in some districts—ten times the WHO's recommended limit—affecting both crop productivity and human health<sup>13,14</sup>.

Evaluating irrigation water quality necessitates sophisticated analytical frameworks that integrate multiple physicochemical parameters<sup>18,20</sup>. Traditional singular metrics like Electrical Conductivity (EC) or Sodium Adsorption Ratio (SAR) provide limited insights, while contemporary approaches such as the Irrigation Water Quality Index (IWQI) enable comprehensive assessment through the mathematical integration of multiple water quality parameters, weighted according to their relative importance for agricultural applications<sup>21–26</sup>. The IWQI methodology has demonstrated particular utility in regions like southern Brazil and northern China, where it has helped identify groundwater bodies unsuitable for irrigation despite meeting individual parameter thresholds<sup>27,28</sup>.

Nitrate contamination represents a critical concern in agricultural groundwater systems with profound implications across multiple ecological dimensions<sup>29–31</sup>. Physiologically, elevated nitrate concentrations can induce oxidative stress in crops, disrupt nutrient uptake mechanisms, and potentially generate phytotoxic nitrite compounds when metabolized under anaerobic conditions<sup>29,31–34</sup>. In Spain's Campo de Dalías region, excessive groundwater nitrate levels (> 50 mg/L) have been directly linked to decreased tomato yields, altered soil microbial communities, and contamination of coastal ecosystems<sup>35</sup>. These impacts extend beyond immediate agricultural concerns, contributing to broader environmental challenges including groundwater-dependent ecosystem degradation<sup>36–38</sup>.

The Hennaya Plain exemplifies the critical intersection of agricultural productivity and water resource vulnerability in semi-arid environments. This region, like many similar agricultural landscapes worldwide, has experienced intensifying groundwater dependency as surface water resources become increasingly unreliable due to climate variability<sup>39,40</sup>. Understanding contamination patterns in such regions has global significance, as similar hydrogeological and agricultural conditions exist across Mediterranean, Middle Eastern, and North African regions<sup>41,44</sup>.

Despite numerous studies examining groundwater quality in agricultural regions, significant knowledge gaps persist regarding the seasonal dynamics of multiple contaminants and their integrated effects on irrigation water suitability. Previous research typically focuses on either isolated quality parameters or single-season assessments, failing to capture the complex temporal variations that characterize groundwater systems in semi-arid agricultural landscapes<sup>42–44</sup>. Additionally, while numerous studies have characterized individual contaminants like nitrates or salts, few have implemented integrated analytical frameworks that simultaneously evaluate multiple quality parameters in relation to irrigation suitability<sup>41,43,44</sup>. This research gap is particularly pronounced in North African agricultural plains, where limited long-term monitoring programs and fragmented data collection efforts have hindered comprehensive understanding of groundwater quality dynamics.

This study introduces a novel integrated approach for irrigation water quality assessment that addresses limitations in conventional methodologies. While previous studies have typically focused on either general water quality indices or specific contaminants, this approach combines comprehensive IWQI analysis<sup>26</sup> with detailed nitrate contamination evaluation. The novelty of this work lies in an integrated methodology that enables simultaneous evaluation of both overall irrigation suitability and specific contamination concerns, providing more nuanced insights than single-parameter or single-index approaches. Furthermore, the seasonal comparative analysis addresses critical gaps in understanding temporal dynamics of groundwater quality in semi-arid agricultural settings. Geographic Information System (GIS) technologies enhance this integration by enabling spatial interpolation of point-based measurements, detection of contamination hotspots, visualization of temporal trends, and identification of correlation patterns between land use and water quality metrics capabilities far beyond traditional statistical analyses<sup>48</sup>.

The research addresses four critical objectives with broad applicability to semi-arid agricultural regions globally: (1) comprehensively assessing groundwater quality using multiple complementary methodologies; (2) quantifying spatial and temporal variations in irrigation water characteristics; (3) establishing a robust framework for sustainable water resource management in agriculturally intensive landscapes; and (4) evaluating potential ecological and agricultural risks associated with current groundwater use patterns. This investigation aims to contribute a more nuanced understanding of groundwater quality challenges in agricultural environments and generate valuable insights for sustainable water resource management applicable across similar hydrogeological and climatic contexts worldwide.

## Materials and methods

### Study area

The Hennaya Plain is situated near of Tlemcen city (North-West Algeria) and extends in a slightly north-south direction (Fig. 1). The plain is delimited by Wadi Isser to the north, the Tlemcen Mountains to the south, Wadi Sikkak to the east, and Wadi Khalouf to the west. The region subjects a semi-arid Mediterranean climate, with monthly temperatures varying from 16.85 to 18.5 °C (average: 17.8 °C) and annual rainfall averaging 395.2 mm. The topography of the Hennaya Plain is predominantly flat, characterized by a gentle slope of approximately 2%, descending from an elevation of 450 m at the southern boundary to approximately 188 m at the northern limit.

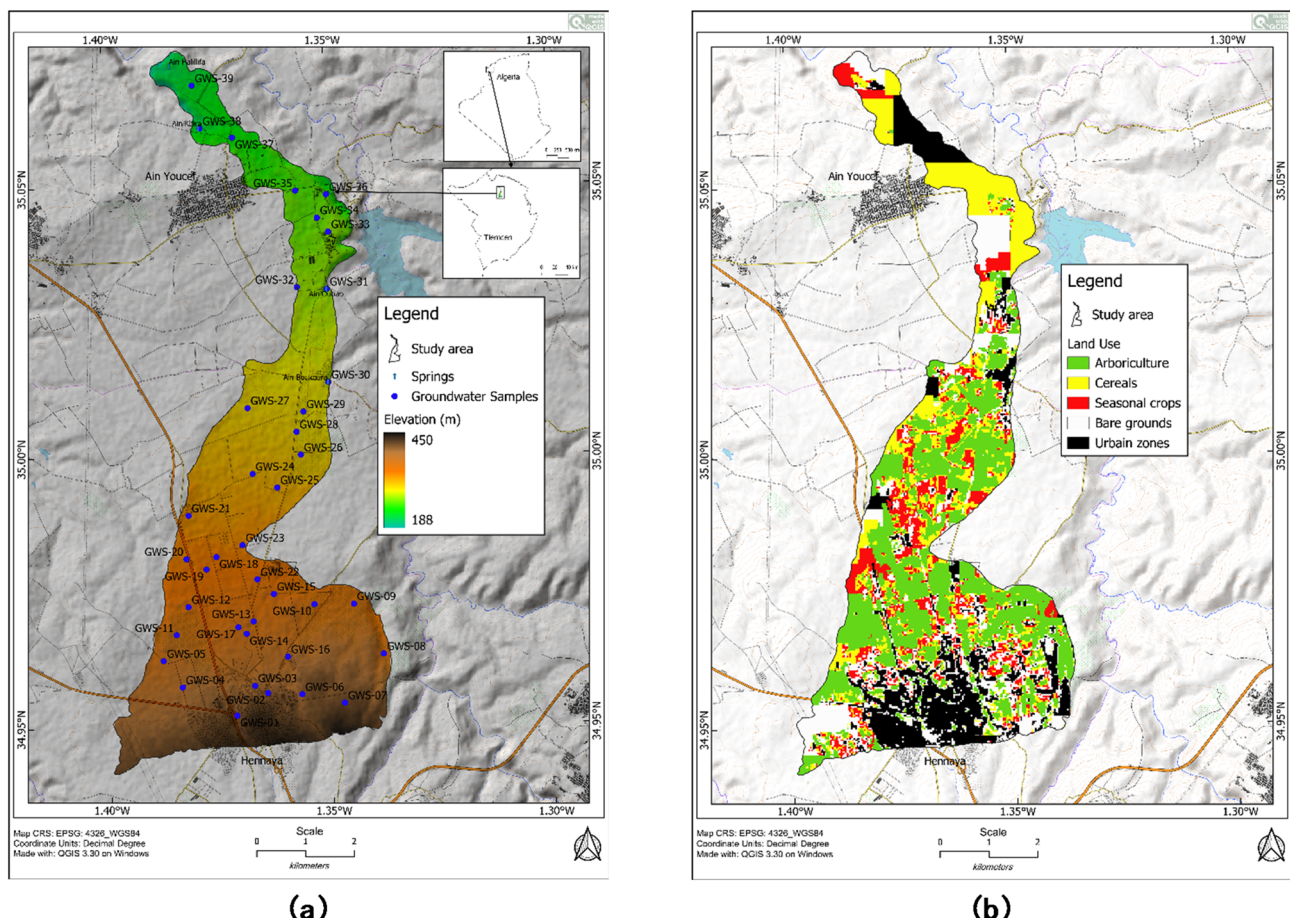


**Fig. 1.** (a) Geographical Context of the Study Area; (b) Land use. Maps were generated using QGIS (version 3.30.1, <https://qgis.org>).

Notably, the slope increases to 2–5% on the dropping cones of river deposits<sup>40,48</sup>. The primary hydrogeological feature in the region is the Mio-Plio-Quaternary aquifer of the Hennaya Plain, which serves as a crucial water source<sup>48</sup> (Fig. 2a). The aquifer is recharged primarily through subsurface flow from the Tlemcen Mountains in the south<sup>48</sup>, complemented by direct precipitation infiltration. However, the aquifer faces several sustainability challenges, including increasing agricultural withdrawals and climate-driven precipitation variability that affects natural replenishment rates. Additionally, the shallow depth of the aquifer in the northern Sect.<sup>39</sup> (Fig. 2b) makes it particularly vulnerable to surface contamination from agricultural activities and urban runoff<sup>48</sup>.

In recent years, the Hennaya Plain has undergone significant agricultural development, with a predominant focus on citrus fruit cultivation (Fig. 1b). This shift in land use and economic activities underscores the growing importance of the region's agricultural sector. Studying this expanded area will provide valuable insights into the intricate interplay between climatic conditions, aquifer dynamics, and the evolving agricultural landscape in the Hennaya Plain.

## Methods

### Groundwater sampling and physicochemical analyses

A comprehensive sampling campaign was conducted across the study area, encompassing thirty-nine ( $n=39$ ) distinct irrigation water sources. Sampling points were strategically selected based on multiple criteria including hydrogeological conditions, land use patterns, agricultural intensity, and proximity to known pollution sources. Site selection was further validated using preliminary field surveys and historical water quality data to ensure representative coverage of the aquifer system. The sampling strategy was designed to capture both seasonal variations during dry (July–August 2023) and wet periods (February–March 2024), as well as spatial heterogeneity, ensuring a representative assessment of the region's water quality dynamics.

This systematic approach ensures that the sampling network effectively captures the spatial variability of water quality parameters across the study area. The investigation focused on 11 key physicochemical parameters: pH, temperature (T), total dissolved solids (TDS), electrical conductivity (EC), magnesium ( $Mg^{2+}$ ), sodium ( $Na^+$ ), calcium ( $Ca^{2+}$ ), chloride ( $Cl^-$ ), bicarbonate ( $HCO_3^-$ ), sulfate ( $SO_4^{2-}$ ), and nitrate-nitrogen ( $NO_3^-$ –N), aiming to provide an overall understanding of water adequacy for irrigation purposes and to characterize groundwater chemistry evolution.

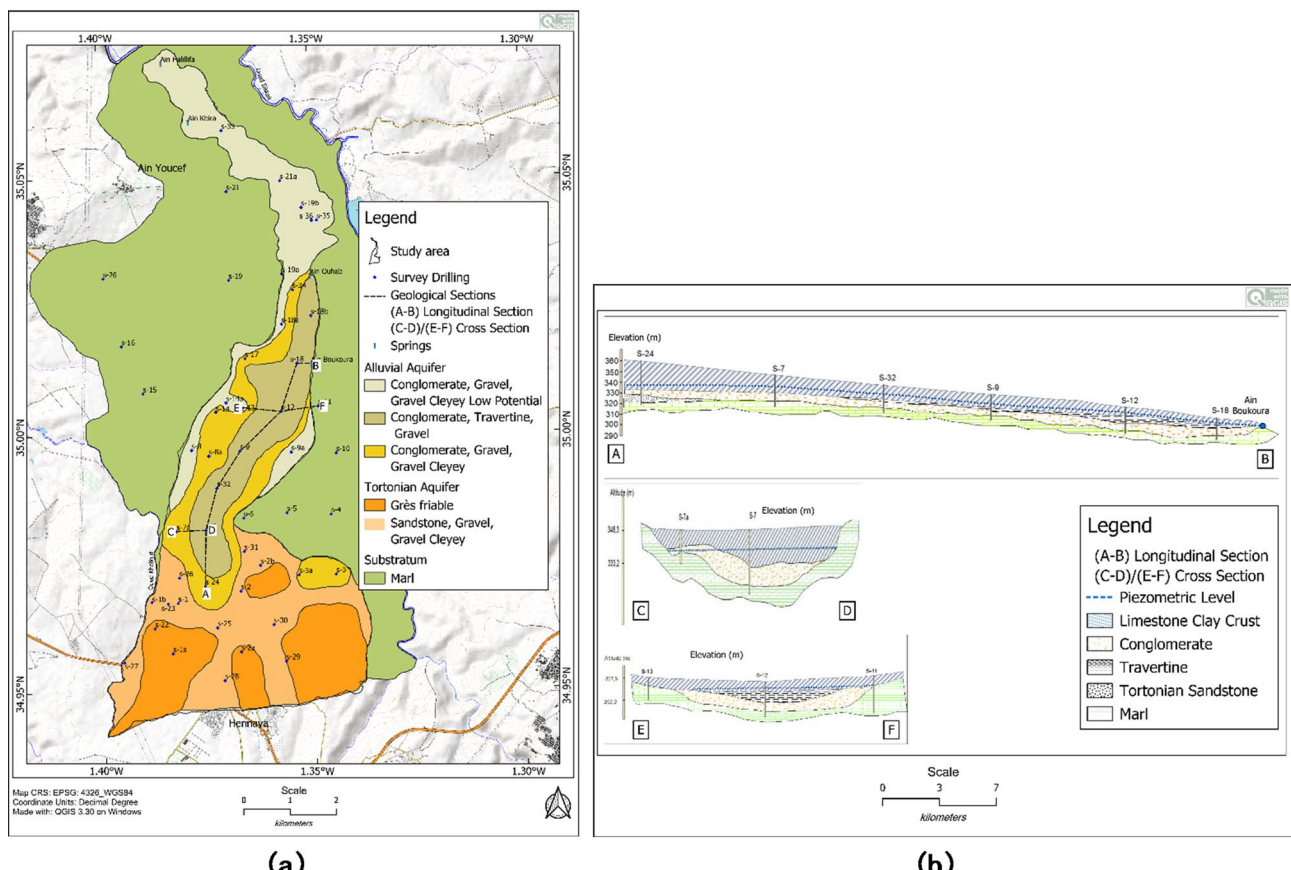


**Fig. 2.** Hydrogeological Context of the Study Area. (a) Hydrogeological Map Describing the Different Aquifer Formations (generated using QGIS version 3.30.1, <https://qgis.org>); (b) Geological Sections of the Aquifer System (created using Inkscape version 1.2, <https://inkscape.org>).

The sampling protocol adhered to standard methods of American Public Health Association (APHA)<sup>49</sup> and involved collection in sterile 250 mL polyethylene vessels, pre-cleaned with deionized water and rinsed three times with sample water before collection. Samples were preserved at 4 °C during transportation and analyzed within 48 h of collection to minimize potential changes in chemical composition. In-situ measurements were conducted for temperature and pH using a calibrated EXTECH pH meter (accuracy  $\pm 0.01$  pH units,  $\pm 0.1$  °C), while EC and TDS were determined using an Isolab Multiparameter analyzer (accuracy  $\pm 1\%$  full scale).

The ionic composition analysis was performed through ion chromatography techniques using METROHM Model 881 compact IC Pro at the National Water Resources Agency's (ANRH) analytical chemistry laboratory, following sample filtration through 0.45 µm PVDF membrane filters. Instrument calibration was performed daily using certified reference standards, and detection limits for analyzed ions ranged from 0.01 to 0.05 mg L<sup>-1</sup> depending on the specific parameter.

Rigorous quality control measures were implemented throughout the analytical process. These included analysis of field blanks, equipment blanks, and trip blanks (one per 10 samples) to assess potential contamination during sampling, transportation, and analysis. Duplicate samples (10% of total samples) were analyzed to evaluate analytical precision, with relative percent differences maintained below 10%. Laboratory control samples and matrix spikes were analyzed to assess accuracy, with recovery percentages between 90 and 110% considered acceptable. The analytical quality was further verified by ensuring that the ionic balance error (Eq. (1)) remained within the acceptable range of  $\leq 5\%$  for all samples<sup>21,50,51</sup>. Certified reference materials from the National Institute of Standards and Technology were analyzed alongside the samples to validate the analytical methodology.

$$CBE = \left[ \frac{\sum (Cations) - \sum (Anions)}{\sum (Cations) + \sum (Anions)} \right] \times 100 \quad (1)$$

#### Data analysis

The analytical data were systematically evaluated against the irrigation water quality guidelines established by the Food and Agriculture Organization of the United Nations (FAO), as detailed in Table 1, providing a

Potential Irrigation Issues			None	Slightly to Moderately	Severely
Salinity	EC	( $\mu\text{S}\cdot\text{cm}^{-1}$ )	< 700	700–3000	> 3000
	TDS	( $\text{mg}\cdot\text{L}^{-1}$ )	< 450	450–2000	> 2000
Infiltrations	SAR 0–3 and	EC=	> 700	700–200	< 200
	SAR 3–6 and	EC=	> 1200	1200–300	< 300
	SAR 6–12 and	EC=	> 1900	1900–500	< 500
	SAR 12–20 and	EC=	> 2900	2900–1300	< 1300
	SAR 20–40 and	EC=	> 5000	5000–2900	< 2900
Specific Ion Toxicities	Sodium ( $\text{Na}^+$ )	SAR	< 3	3–9	> 9
	Chloride ( $\text{Cl}^-$ )	( $\text{mg}\cdot\text{L}^{-1}$ )	< 140	140–350	> 350
Miscellaneous Impacts	Nitrate-nitrogen ( $\text{NO}_3\text{---N}$ )	( $\text{mg}\cdot\text{L}^{-1}$ )	< 5	5–30	> 30
	Bicarbonate ( $\text{HCO}_3^-$ )	( $\text{mg}\cdot\text{L}^{-1}$ )	< 91.5	91.5–518.5	> 518.5
	pH	Normal range	6.5–8.5		

**Table 1.** Guideline of irrigation water quality<sup>31</sup>. The Sodium Adsorption Ratio (SAR) serves as a critical indicator for assessing the potential soil structural degradation associated with irrigation practices. This parameter quantifies the relative proportions of sodium ions to calcium and magnesium ions in the water samples<sup>52–54</sup>. Elevated SAR values indicate sodium predominance, which can adversely affect soil physical properties, including structural stability, hydraulic conductivity, and infiltration capacity, ultimately impacting agricultural productivity<sup>45–47,55,56</sup>. The SAR values were calculated using the established Eq. (2) proposed by Wilcox<sup>53</sup> (as cited in<sup>54</sup>):

standardized framework for systematic assessment of water quality parameters and their potential impacts on agricultural applications.

$$SAR = \frac{\text{Na}^+}{\sqrt{(\text{Ca}^{2+} + \text{Mg}^{2+})/2}} \quad (2)$$

where all ion concentrations expressed in ( $\text{meq}\cdot\text{L}^{-1}$ ).

The research methodology integrated multiple advanced analytical approaches to comprehensively evaluate irrigation water quality. Spatial data visualization and interpolation were conducted using QGIS (version 3.30.1, <https://qgis.org>). Ordinary Kriging was selected as the optimal interpolation method due to its unique advantages for groundwater quality assessment: (1) it accounts for the natural spatial continuity of hydrogeological parameters through variogram analysis, (2) provides uncertainty quantification through kriging variance, and (3) incorporates directional trends in groundwater flow through anisotropic modeling. The method's implementation involved rigorous variogram analysis and model selection through cross-validation, ensuring robust spatial predictions while maintaining physical meaningfulness<sup>59,60</sup>.

#### Statistical methods

The hydrochemical data analysis employed three complementary statistical approaches for geochemical interpretation. Pearson correlation matrices were used to identify significant linear relationships between parameters, with correlation coefficients ( $r$ ) indicating strength and direction of associations between geochemical variables ( $p < 0.05$ )<sup>61</sup>. Principal Component Analysis (PCA) reduced dataset dimensionality while maximizing variance explanation, transforming correlated variables into uncorrelated principal components; the resulting biplots displayed both variable loadings and sample scores on the first two factorial planes, facilitating identification of dominant geochemical processes and spatial patterns<sup>45–47</sup>. Hierarchical Cluster Analysis (HCA) using Euclidean distance and Ward's minimum variance method identified natural groupings among parameters, represented as dendograms with dissimilarity thresholds. This approach revealed parameter associations and geochemical process integration across different conditions, providing insights into the relationships between water quality variables and underlying hydrogeochemical mechanisms<sup>61,62</sup>. This analysis was performed using XLSTAT.

#### Irrigation water quality index (IWQI)

The Irrigation Water Quality Index (IWQI) is a comprehensive quantitative approach designed to evaluate the suitability of water resources for agricultural irrigation<sup>26</sup>. This index integrates multiple water quality parameters into a single numerical value, providing a holistic assessment of water quality that can guide irrigation management decisions.

The IWQI incorporates critical water quality parameters, including Electrical Conductivity (EC), Sodium Adsorption Ratio (SAR), Sodium concentration, Chloride concentration, and Bicarbonate concentration. These parameters were carefully selected to capture the various chemical and physical characteristics that potentially impact crop growth and soil health<sup>63,64</sup>. This index is calculated using a weighted aggregation methodology (Eq. 3)<sup>26</sup>:

qi	EC ( $\mu\text{S.cm}^{-1}$ )	SAR	$\text{Na}^+$ ( $\text{mg.L}^{-1}$ )	$\text{Cl}^-$ ( $\text{mg.L}^{-1}$ )	$\text{HCO}_3^-$ ( $\text{mg.L}^{-1}$ )
85–100	$200 \leq \text{EC} < 750$	$\text{SAR} < 3$	$2 \leq \text{Na}^+ < 3$	$\text{Cl}^- < 4$	$1 \leq \text{HCO}_3^- < 1.5$
60–85	$750 \leq \text{EC} < 1500$	$3 \leq \text{SAR} < 6$	$3 \leq \text{Na}^+ < 6$	$4 \leq \text{Cl}^- < 7$	$1.5 \leq \text{HCO}_3^- < 4.5$
35–60	$1500 \leq \text{EC} < 3000$	$6 \leq \text{SAR} < 12$	$6 \leq \text{Na}^+ < 9$	$7 \leq \text{Cl}^- < 10$	$4.5 \leq \text{HCO}_3^- < 8.5$
0–35	$\text{EC} < 200 \text{ or } \text{EC} \geq 3000$	$\text{SAR} \geq 12$	$\text{Na}^+ < 2 \text{ or } \text{Na}^+ \geq 9$	$\text{Cl}^- \geq 10$	$\text{HCO}_3^- < 1 \text{ or } \text{HCO}_3^- \geq 8.5$

**Table 2.** Parameter's values for the sub-index ( $qi$ ) measurement calculation<sup>26</sup>.

Parameters	Weight ( $wi$ )
EC	0.211
SAR	0.204
$\text{Na}^+$	0.202
$\text{Cl}^-$	0.194
$\text{HCO}_3^-$	0.189

**Table 3.** Weights assigned ( $wi$ ) to parameters<sup>26</sup>.

$$IWQI = \sum_{i=1}^n wi \bullet qi \quad (3)$$

where  $wi$  represents the weight of each parameter, and  $qi$  represents the sub-index value.

The sub-index ( $qi$ ) calculation method involves transforming each water quality parameter into a standardized (Table 2) value using the following equation (Eq. (4))<sup>26,64,65</sup>:

$$qi = (qi) \text{ max} - \left[ (xij - xinf) \times \frac{(qi) \text{ amp}}{x \text{ amp}} \right] \quad (4)$$

where  $(qi) \text{ max}$  is the highest possible  $qi$  value for the category of particular  $i$  parameter, the variable  $xij$  is the actual measured value of the parameter in a water sample,  $xinf$  denotes the lower limit of the parameter's designated class,  $(qi) \text{ amp}$  represents the full range of values for the parameter within its defined grading class, calculated by determining the difference between the highest and lowest permissible values, and  $x \text{ amp}$  is the class amplitude to which the factor belongs.

The weights  $wi$  represents the normalized values assigned to various water parameters<sup>26</sup>. These weights are calculated for each factor to reflect their relative impact on water quality. Table 3 exhibits the weighting of IWQI factors.

The IWQI represents a dimensionless measure varying from 0 to 100 and is classified into 5 classes defined according to specific ranges of IWQI values, taking into account the salinity issue risk, decline in water penetration into the soil, and toxicity to plants<sup>26,66</sup>.

Interpretation of the IWQI follows structured guidelines: values below 55 indicate water unsuitable for irrigation and requiring significant remediation, values between 55 and 70 suggest conditional suitability with careful management needed, and values of 70 or above represent highly suitable irrigation water with minimal constraints.

Importantly, the methodology acknowledges its own limitations. Regular recalibration of parameter weights is recommended to account for changing local agricultural conditions. Additionally, the index should be used in conjunction with supplementary assessments of specific crop tolerances and considerations of seasonal variations in water quality. This approach ensures a dynamic and context-sensitive evaluation of irrigation water resources.

#### Integrated IWQI and $\text{NO}_3^-$ -N

This study presents a comprehensive methodological framework for assessing irrigation groundwater quality through the integration of two critical parameters: the Irrigation Water Quality Index (IWQI) and nitrate concentration levels. The methodology was implemented in the Hennaya Plain region, an area characterized by significant groundwater nitrogen contamination<sup>39</sup>. The assessment framework employs a dual-criteria classification system that combines spatial distribution analysis of both IWQI values and nitrate-nitrogen ( $\text{NO}_3^-$ -N) concentrations to determine water quality categories. Importantly, this approach adopts a conservative assessment principle where the final classification is always determined by the most restrictive criterion between IWQI and nitrate concentration.

The classification system operates through a hierarchical decision matrix based on the following criteria:

1. Unsuitable Quality: Defined by either  $IWQI < 55$  OR  $NO_3^-N > 30 \text{ mg.L}^{-1}$  (the presence of either unsuitable condition leads to an unsuitable classification).
2. Moderate Quality: Occurs in two scenarios:
  - When  $IWQI$  is between 55 and 70 AND  $NO_3^-N \leq 30 \text{ mg.L}^{-1}$ ;
  - When  $IWQI > 70$  AND  $NO_3^-N$  is between 5 and 30  $\text{mg.L}^{-1}$ .
3. Good Quality: Requires concurrent achievement of two conditions:
  - $IWQI > 70$  AND;
  - $NO_3^-N < 5 \text{ mg.L}^{-1}$  (both criteria must be met for good quality classification).

This integrated approach provides a more robust evaluation framework compared to single-parameter assessments, incorporating both general irrigation water quality parameters (through  $IWQI$ ) and specific nitrogen pollution indicators, always defaulting to the most conservative assessment. The following flowchart illustrates the systematic decision-making process of this assessment methodology (Fig. 3):

## Results

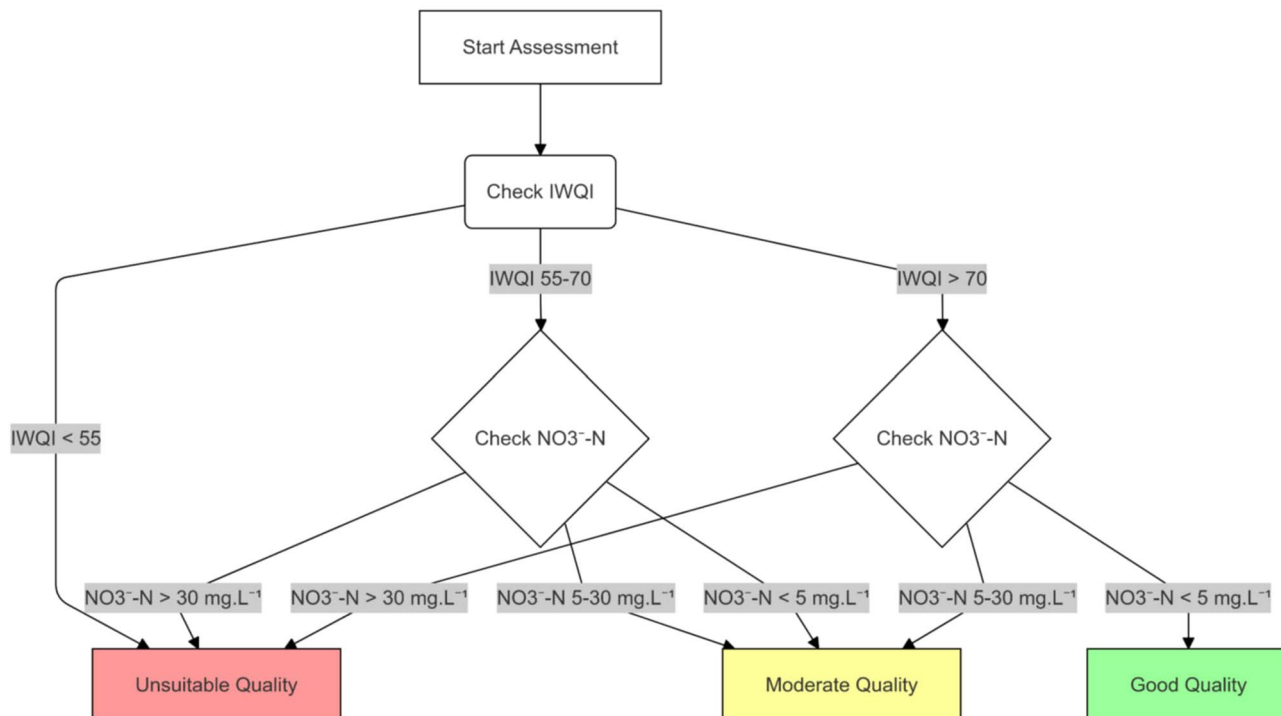
### General physicochemical characteristics

Table 4 presents the descriptive statistical analysis of physical parameters and chemical elements (cations and anions) in groundwater samples from the Hennaya plain during dry and wet periods, including maximum values, minimum values, means, standard deviations, and coefficients of variation.

Groundwater samples from the study area displayed distinct physicochemical patterns across seasons. pH values remained near-neutral (7.15–8.41) with decreased variability during wet conditions (coefficient of variation: 5.04–2.05%). This slight alkalinity likely reflects influences from carbonate minerals and local geological formations. Total Dissolved Solids (TDS) and Electrical Conductivity (EC) decreased during wet periods from means of 1272.18 to 1166.11  $\text{mg.L}^{-1}$  and 1631 to 1495  $\mu\text{S.cm}^{-1}$ , respectively, suggesting dilution effects from precipitation and enhanced groundwater recharge. The moderate variation indicates a stable hydrochemical system with effective buffering capacity.

### Seasonal variation in major cations

The major cation composition showed marked seasonal changes, with different elements responding distinctly to hydrological conditions. Sodium concentrations decreased dramatically from a maximum of 450.6  $\text{mg.L}^{-1}$  in dry conditions to 150.66  $\text{mg.L}^{-1}$  during wet periods, with variation coefficients declining from 24.65 to 7.92%. This significant shift likely results from seasonal ion exchange processes and hydrological mixing that particularly affect sodium mobility in the aquifer system. In contrast, calcium and magnesium concentrations



**Fig. 3.** Flowchart Illustrating the Proposed Methodology for Comprehensive Assessment of the Groundwater's physicochemical Quality.

Parameters	Min		Max		Mean		Standard Deviation		Coefficient of Variation (%)	
	Dry	Wet	Dry	Wet	Dry	Wet	Dry	Wet	Dry	Wet
	14.5	16.2	20.6	23.7	18.5	19.25	1.92	2.18	10.38	11.32
pH	7.15	7.12	8.41	7.68	7.63	7.31	0.38	0.15	5.04	2.05
TDS (mg.L <sup>-1</sup> )	1093.56	1060.02	1443	1281.5	1272.18	1166.11	93.92	61.51	7.38	5.27
EC (μS.cm <sup>-1</sup> )	1402	1359	1850	1643	1631	1495	120.41	78.86	7.38	5.27
Na <sup>+</sup> (mg.L <sup>-1</sup> )	139.55	113.30	450.6	150.66	217.15	135.09	53.53	10.71	24.65	7.92
Ca <sup>2+</sup> (mg.L <sup>-1</sup> )	110.64	112.20	228.02	247.25	140.75	142.3	17.66	19.47	12.54	13.68
Mg <sup>2+</sup> (mg.L <sup>-1</sup> )	52.34	52.6	96.48	98.45	80.3	77.36	8.53	10.01	10.62	12.93
Cl <sup>-</sup> (mg.L <sup>-1</sup> )	133.56	130.25	915.2	545.6	303.53	263.42	188.62	89.5	62.14	37.86
SO <sub>4</sub> <sup>2-</sup> (mg.L <sup>-1</sup> )	83	84.57	181.65	178.77	120.5	119.6	23.49	22.88	19.5	19.13
HCO <sub>3</sub> <sup>-</sup> (mg.L <sup>-1</sup> )	345.51	351.21	552.21	550.25	442.69	439.53	64.78	63.13	14.63	14.37
NO <sub>3</sub> <sup>-</sup> -N (mg.L <sup>-1</sup> )	12.79	22.14	45.56	49.08	24.06	32.36	6.94	5.99	28.86	18.51

**Table 4.** Statistical overview of groundwater physicochemical parameters in Hennaya plain.

remained relatively stable (variation coefficients: 10.62–13.68%), indicating consistent mineral-water interactions throughout the seasons<sup>67</sup>.

#### Anion dynamics across seasons

Among anions, chloride demonstrated the greatest variability, with concentrations ranging from 133.56 to 915.2 mg.L<sup>-1</sup> during dry conditions to 130.25–545.6 mg.L<sup>-1</sup> in wet periods. The variation coefficient decreased from 62.14 to 37.86%, reflecting complex interactions between geological sources, potential anthropogenic inputs, seasonal precipitation patterns, and groundwater dynamics. Unlike chloride's pronounced variability, sulfate and bicarbonate maintained consistent mean concentrations with low variation coefficients, suggesting chemical stability and effective buffering mechanisms within the water system<sup>68,69</sup>.

#### Nitrogen compounds and agricultural influence

Beyond the major ions discussed above, nitrate-nitrogen concentrations also showed seasonal patterns that merit specific attention. Concentrations ranged from 12.79 to 49.08 mg.L<sup>-1</sup>, with moderate seasonal variations (variation coefficients: 28.86% in dry periods, 18.51% in wet conditions). These variations potentially indicate agricultural inputs and nitrogen cycle dynamics influenced by seasonal changes in precipitation and groundwater recharge<sup>32</sup>.

This comprehensive analysis reveals complex hydrogeochemical processes within the Hennaya plain aquifer system. The seasonal variations, particularly in sodium and chloride concentrations, indicate sensitivity to environmental changes, while stable pH values and consistent behavior of certain ions suggest underlying geochemical buffering mechanisms. These findings highlight the importance of temporal monitoring to understand groundwater dynamics in the region<sup>70</sup>. The observed patterns reflect both natural hydrogeological processes and potential anthropogenic influences, including agricultural activities and urban development in the region.

#### Sources identification of dissolved ions using multivariate statistical analysis

To better understand the hydrogeochemical processes and identify the potential sources of dissolved ions in the Hennaya plain groundwater, multivariate statistical techniques including Principal Component Analysis (PCA) and correlation analysis were applied to the hydrochemical data collected during both dry and wet seasons. These techniques help in determining the relationships between various physicochemical parameters and identifying the dominant factors controlling groundwater quality and the origin of contamination.

#### Correlation analysis

The correlation analysis (Table 5) showed significant relationships between the physicochemical parameters across both seasons. TDS and EC showed a perfect positive correlation ( $r=1.000$ ) in both seasons, confirming that dissolved ions are the primary contributors to electrical conductivity. The relationship between TDS and Na<sup>+</sup> was moderate in the dry season ( $r=0.620$ ) and remained substantial in the wet season ( $r=0.576$ ), suggesting consistent influence of sodium salts on groundwater mineralization throughout the year. Notably, the correlation between TDS and pH varied considerably between seasons, with a moderate positive correlation in the dry season ( $r=0.519$ ) strengthening significantly during the wet season ( $r=0.714$ ), indicating enhanced mineral dissolution during rainfall events.

Chloride showed interesting seasonal variations in its relationships with other parameters. In the dry season, Cl<sup>-</sup> exhibited strong correlation with TDS ( $r=0.714$ ) and moderate correlation with Na<sup>+</sup> ( $r=0.521$ ) and NO<sub>3</sub><sup>-</sup>-N ( $r=0.491$ ), suggesting common sources. However, in the wet season, Cl<sup>-</sup> showed negligible correlation with TDS ( $r=0.009$ ) while maintaining significant correlations with Na<sup>+</sup> ( $r=0.515$ ) and developing stronger associations

Variables	T	pH	TDS	EC	Na <sup>+</sup>	Ca <sup>2+</sup>	Mg <sup>2+</sup>	Cl <sup>-</sup>	SO <sub>4</sub> <sup>-2</sup>	HCO <sub>3</sub> <sup>-</sup>	NO <sub>3</sub> <sup>-</sup> -N
Dry											
T	<b>1</b>										
pH	0.213	<b>1</b>									
TDS	0.290	<b>0.519</b>	<b>1</b>								
EC	0.182	<b>0.518</b>	<b>1.000</b>	<b>1</b>							
Na <sup>+</sup>	0.159	0.164	<b>0.620</b>	0.120	<b>1</b>						
Ca <sup>2+</sup>	-0.034	-0.170	-0.151	-0.150	0.118	<b>1</b>					
Mg <sup>2+</sup>	-0.007	0.164	0.096	0.093	-0.053	-0.204	<b>1</b>				
Cl <sup>-</sup>	0.222	0.311	<b>0.714</b>	-0.014	<b>0.521</b>	0.245	-0.394	<b>1</b>			
SO <sub>4</sub> <sup>-2</sup>	0.229	0.109	0.392	0.292	0.252	0.038	-0.070	0.096	<b>1</b>		
HCO <sub>3</sub> <sup>-</sup>	-0.360	-0.646	-0.483	-0.483	-0.209	0.068	0.068	-0.318	-0.376	<b>1</b>	
NO <sub>3</sub> <sup>-</sup> -N	0.081	-0.310	0.311	-0.310	0.160	0.381	-0.456	<b>0.491</b>	0.173	0.158	<b>1</b>
Wet											
T	<b>1</b>										
pH	0.424	<b>1</b>									
TDS	0.149	<b>0.714</b>	<b>1</b>								
EC	0.149	<b>0.714</b>	<b>1.000</b>	<b>1</b>							
Na <sup>+</sup>	0.019	0.319	<b>0.576</b>	0.576	<b>1</b>						
Ca <sup>2+</sup>	0.106	-0.153	-0.159	-0.159	0.198	<b>1</b>					
Mg <sup>2+</sup>	-0.093	0.316	0.225	0.225	-0.083	-0.245	<b>1</b>				
Cl <sup>-</sup>	0.112	-0.122	0.009	0.009	<b>0.515</b>	0.408	-0.430	<b>1</b>			
SO <sub>4</sub> <sup>-2</sup>	0.170	0.221	0.381	0.381	0.423	0.073	-0.044	0.446	<b>1</b>		
HCO <sub>3</sub> <sup>-</sup>	-0.078	-0.419	-0.630	-0.630	-0.645	0.033	-0.052	-0.333	-0.352	<b>1</b>	
NO <sub>3</sub> <sup>-</sup> -N	<b>0.559</b>	-0.05	<b>0.601</b>	<b>0.612</b>	<b>0.499</b>	0.417	<b>0.588</b>	<b>0.577</b>	0.723	-0.463	<b>1</b>

**Table 5.** Correlation matrix of physicochemical parameters of groundwater.

with NO<sub>3</sub><sup>-</sup>-N ( $r=0.577$ ) and Ca<sup>2+</sup> ( $r=0.408$ ), indicating a shift in hydrochemical processes and possibly enhanced anthropogenic inputs during the rainy period.

Nitrate correlations exhibited the most dramatic seasonal changes, reflecting its dynamic behavior in groundwater. In the dry season, NO<sub>3</sub><sup>-</sup>-N showed moderate positive correlation with Cl<sup>-</sup> ( $r=0.491$ ) and Ca<sup>2+</sup> ( $r=0.381$ ), with a negative relationship with Mg<sup>2+</sup> ( $r=-0.456$ ). During the wet season, NO<sub>3</sub><sup>-</sup>-N developed strong positive correlations with multiple parameters including SO<sub>4</sub><sup>-2</sup> ( $r=0.723$ ), TDS/EC ( $r \approx 0.60$ ), Na<sup>+</sup> ( $r=0.499$ ), Cl<sup>-</sup> ( $r=0.577$ ), and even Mg<sup>2+</sup> ( $r=0.588$ ), suggesting widespread nitrate contamination during rainfall events due to increased leaching of agricultural fertilizers.

Bicarbonate consistently showed negative correlations with most parameters across both seasons, with particularly strong negative associations with pH in the dry season ( $r = -0.646$ ) and with TDS/EC ( $r = -0.630$ ) and Na<sup>+</sup> ( $r = -0.645$ ) in the wet season, indicating that carbonate dissolution processes are inversely related to overall mineralization, possibly due to competing ion effects or dilution during recharge events.

#### Principal component analysis (PCA)

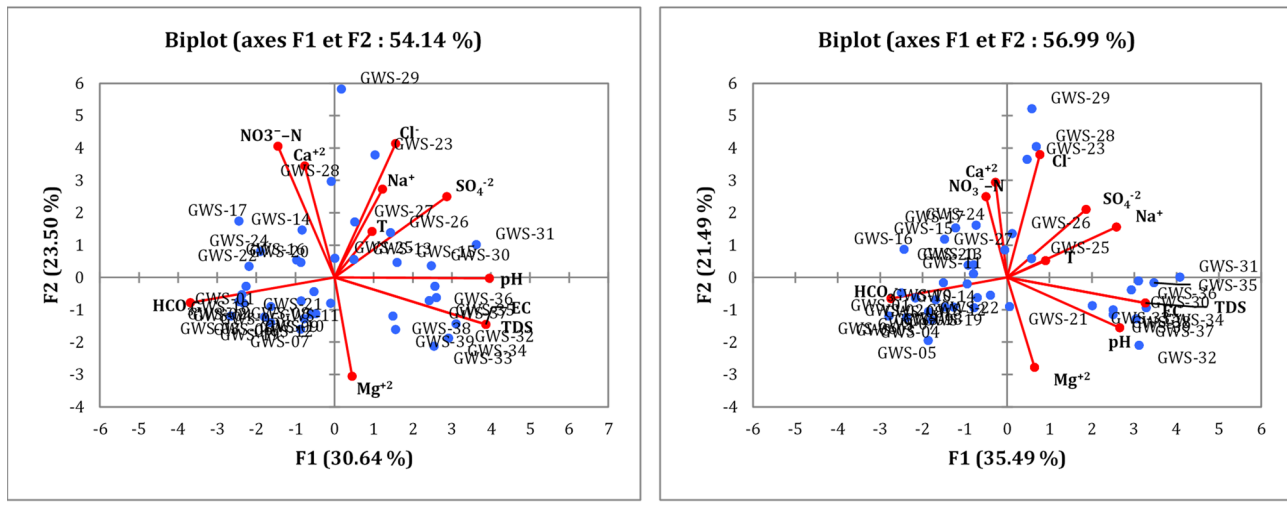
PCA was performed to identify the major factors controlling groundwater chemistry during both dry and wet seasons. Five principal components were extracted in each case, collectively explaining approximately 83.5% of the variance in the dry season and 84.3% in the wet season (Table 6).

*Factor 1 (F1)* emerged as the dominant component, explaining 30.6% of the variance in the dry season and 35.5% in the wet season. This factor primarily represents mineral dissolution processes and natural geochemical evolution of groundwater. In both seasons, F1 showed strong positive loadings for TDS (0.820–0.929), EC (0.819–0.929), and pH (0.839–0.756), with strong negative loadings for HCO<sub>3</sub><sup>-</sup> (-0.780 to -0.781). This consistent pattern indicates the significant influence of water-rock interactions throughout the year. Notably, NO<sub>3</sub><sup>-</sup>-N exhibited contrasting behavior, with a negative loading in the dry season (-0.306) transforming to a strong positive loading in the wet season (0.742), suggesting that nitrate becomes a significant component of the mineral content during rainfall events due to increased leaching.

*Factor 2 (F2)*, explaining 23.5% and 21.5% of the variance in dry and wet seasons respectively, primarily represented anthropogenic pollution sources. This factor maintained strong positive loadings for Cl<sup>-</sup> (0.766–0.841), Ca<sup>2+</sup> (0.638–0.651), and NO<sub>3</sub><sup>-</sup>-N (0.752–0.554) across both seasons, with consistent negative loadings for Mg<sup>2+</sup> (-0.567 to -0.616). This pattern confirms the year-round influence of agricultural activities involving nitrogen fertilizers. The stability of this factor across seasons suggests persistent anthropogenic pressure on the aquifer system.

*Factor 3 (F3)*, accounting for 12.8% and 10.9% of the variance in dry and wet seasons respectively, showed the most dramatic seasonal contrast. Temperature exhibited strong but opposite loadings between dry (-0.712) and wet (0.803) seasons. This reversal highlights the significant impact of seasonal climatic variations on groundwater

Factors	F1		F2		F3		F4		F5	
	Dry	Wet								
T	0.303	0.259	0.263	0.114	-0.712	<b>0.803</b>	0.241	-0.433	-0.436	-0.100
pH	<b>0.839</b>	<b>0.756</b>	-0.005	-0.344	-0.194	0.352	0.143	-0.175	0.132	0.088
TDS	<b>0.820</b>	<b>0.929</b>	-0.270	-0.174	0.380	0.004	-0.214	0.099	-0.111	0.020
EC	<b>0.819</b>	<b>0.929</b>	-0.269	-0.174	0.380	0.004	-0.215	0.099	-0.111	0.020
Na <sup>+</sup>	<b>0.600</b>	0.735	<b>0.505</b>	0.344	<b>0.469</b>	-0.373	<b>0.509</b>	-0.135	-0.044	0.138
Ca <sup>2+</sup>	-0.161	-0.078	<b>0.638</b>	<b>0.651</b>	0.288	0.119	0.323	-0.134	-0.213	<b>0.699</b>
Mg <sup>2+</sup>	0.095	0.184	-0.567	-0.616	-0.050	0.095	0.673	0.446	0.262	0.398
Cl <sup>-</sup>	0.330	0.219	<b>0.766</b>	<b>0.841</b>	<b>0.484</b>	-0.133	-0.117	-0.102	0.279	-0.093
SO <sub>4</sub> <sup>-2</sup>	<b>0.608</b>	0.531	0.463	0.465	-0.174	0.161	-0.020	0.406	<b>0.473</b>	-0.292
HCO <sub>3</sub> <sup>-</sup>	-0.780	-0.781	-0.145	0.144	0.206	0.276	-0.027	0.052	0.354	0.027
NO <sub>3</sub> <sup>-</sup> -N	-0.306	<b>0.742</b>	<b>0.752</b>	<b>0.554</b>	0.089	<b>0.491</b>	-0.220	<b>0.608</b>	-0.025	0.017
Eigenvalues	3.37	3.904	2.585	2.364	1.408	1.204	1.050	1.021	0.776	0.780
Variability (%)	30.642	35.493	23.497	21.493	12.796	10.944	9.549	9.285	7.058	7.093
% cumulative	30.642	35.493	54.139	56.986	66.935	67.930	76.484	77.216	83.542	84.309

**Table 6.** Factorial loadings of extracted eigenvalues in PCA.**Fig. 4.** Projections of variables and individuals on factorial axes PC1-PC2. (a) Dry Season ; (b) wet Season.

thermal dynamics and associated hydrochemical processes, including reaction rates and microbial activity that may influence contaminant transformation.

Factors 4 and 5 (F4, F5) explained smaller portions of the variance (9.5% and 7.1% in the dry season; 9.3% and 7.1% in the wet season) and showed variable patterns between seasons, representing more localized or intermittent influences on groundwater chemistry. Factor 4 showed moderate loadings for Mg<sup>2+</sup> in both seasons (0.673 in dry and 0.446 in wet), while Factor 5 exhibited notable loadings for Ca<sup>2+</sup> (0.699) in the wet season.

#### Projection on factorial plane CP1-CP2

In both seasons, the F1-F2 factorial plane explains a substantial portion of total variance (54.14% in dry season vs. 56.99% in wet season). The F1 axis consistently shows strong positive loadings for EC and TDS (0.819/0.820 in dry season; both 0.929 in wet season), confirming their dominant role in groundwater mineralization. pH maintains significant positive loadings on F1 across seasons (0.839 in dry, 0.756 in wet), while HCO<sub>3</sub><sup>-</sup> shows persistent strong negative loadings (-0.780 in dry, -0.781 in wet) (Fig. 4).

The most notable seasonal shift occurs with NO<sub>3</sub><sup>-</sup>-N, which transitions from primarily associating with F2 (anthropogenic sources) in the dry season (0.752) to showing stronger association with F1 (0.742) in the wet season. This indicates rainfall events significantly enhance nitrate mobilization, integrating this contaminant into the overall mineralization pattern. The F2 axis remains primarily defined by Cl<sup>-</sup> and Ca<sup>2+</sup> in both seasons, though with varying loadings.

Sample distribution patterns change significantly between seasons. During the dry season, GWS-22 appears as an outlier with high F2 scores indicating anthropogenic pollution, while GWS-31, GWS-34, and GWS-35 show high F1 scores suggesting enhanced natural mineralization (Fig. 4a). In contrast, the wet season reveals extreme pollution hotspots at GWS-29, GWS-28, and GWS-27 with very high F2 scores (5.1, 3.9, and 3.8 respectively), while GWS-35, GWS-36, and GWS-31 exhibit high F1 scores (Fig. 4b). The increased variance explained in the wet season and greater sample dispersion suggest that recharge events amplify differences in mineralization patterns across the study area.

#### Hierarchical cluster analysis (HCA)

The hierarchical cluster analysis shows significant structural changes between seasons (Fig. 5). In the dry season (dissimilarity level  $\sim 1.6$ ), three main clusters form: (1) TDS, EC, T, pH and  $\text{SO}_4^{2-}$  form a group defining overall groundwater characteristics; (2) a cluster containing two subgroups - one representing salinization processes ( $\text{Na}^+$ ,  $\text{Cl}^-$ ) and another representing agricultural influence ( $\text{Ca}^{+2}$ ,  $\text{NO}_3^-$ -N); and (3) a couple ( $\text{HCO}_3^-$ ,  $\text{Mg}^{+2}$ ) remains completely separate (Fig. 5a).

The wet season dendrogram (dissimilarity level  $\sim 1.2$ ) (Fig. 5b) shows a modified pattern: TDS and EC maintain their close association with pH, but this association now clusters with  $\text{Mg}^{+2}$ . A more complex cluster emerges including  $\text{SO}_4^{2-}$ ,  $\text{NO}_3^-$ -N,  $\text{Cl}^-$ ,  $\text{Ca}^{+2}$ , and  $\text{Na}^+$ , indicating more integrated hydrochemical processes. While  $\text{HCO}_3^-$  continues to show distinct behavior, it forms connections at a lower dissimilarity level than in the dry season.

The most notable seasonal difference is the reorganization of  $\text{NO}_3^-$ -N,  $\text{Cl}^-$ , and  $\text{Ca}^{+2}$  associations, showing tighter integration with other parameters during the wet season. The lower overall dissimilarity levels in the wet season indicate greater parameter integration, likely due to the homogenizing effect of recharge waters. Additionally, pH's shifting position between seasons reflects changes in mineral dissolution processes under different hydrological conditions. These changes demonstrate how seasonal hydrological variations fundamentally alter the interactions between dissolved ions in groundwater, highlighting the importance of temporal monitoring for comprehensive hydrochemical characterization of the Hennaya plain.

#### Evaluation of irrigation water quality based on FAO standards

The groundwater quality assessment provided comprehensive insights into the physicochemical characteristics across two distinct sampling periods (dry and rainy seasons), evaluated against current Food and Agriculture Organization (FAO) irrigation water standards<sup>31</sup>. Figure 4 presents the descriptive statistical analysis of key water quality parameters, highlighting seasonal variations.

#### pH and electrical properties

pH levels demonstrated minimal seasonal variation, with mean values of 7.63 during the dry period and 7.31 during the rainy season (Fig. 6a). These values consistently fell within the optimal range recommended by FAO guidelines for irrigation water. Electrical conductivity (EC) (Fig. 6b) and total dissolved solids (TDS) (Fig. 6c) exhibited similar seasonal patterns, with higher concentrations during the dry period (1631  $\mu\text{S}\cdot\text{cm}^{-1}$  and 1272.18  $\text{mg}\cdot\text{L}^{-1}$ , respectively) compared to the rainy season (1495  $\mu\text{S}\cdot\text{cm}^{-1}$  and 1166.11  $\text{mg}\cdot\text{L}^{-1}$ , respectively). This seasonal reduction can be attributed to dilution effects from precipitation during the rainy season.

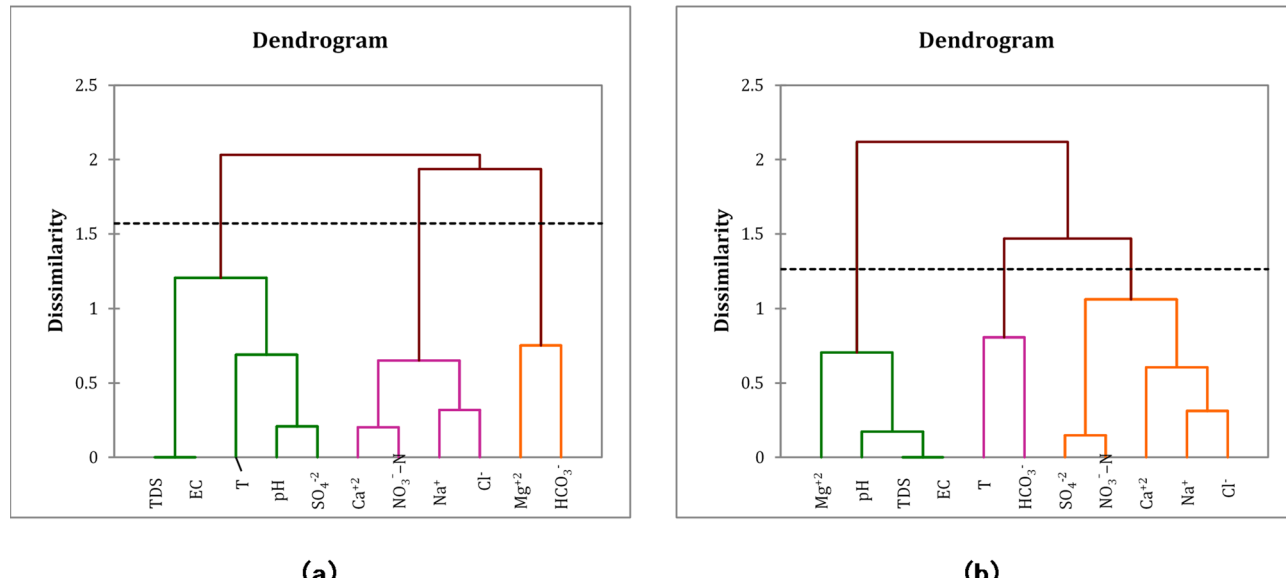


**Fig. 5.** Dendrograms of variable classes. **(a)** Dry Season ; **(b)** wet Season.

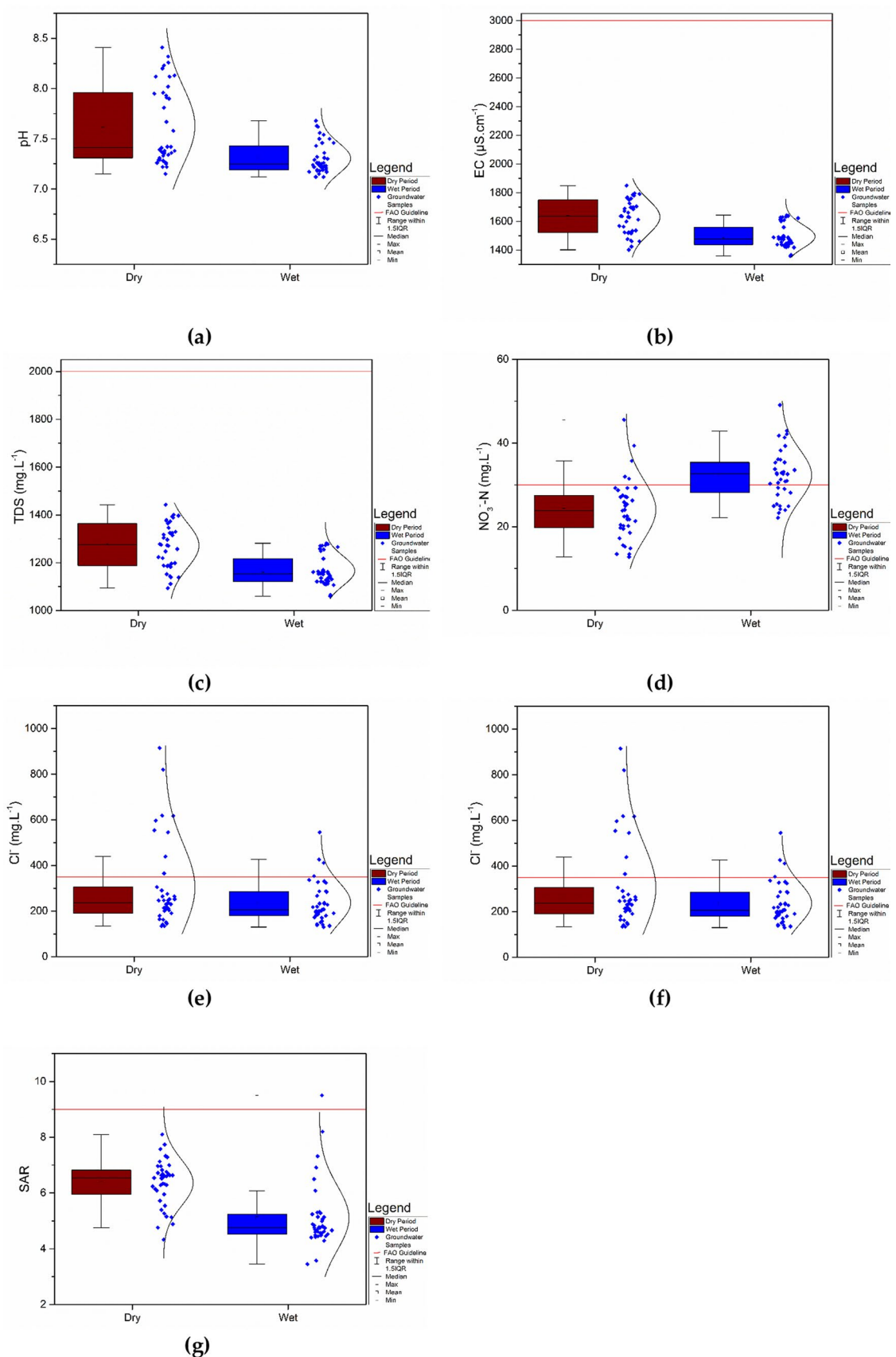


**Fig. 6.** Box Plots Showing the Distribution and Exceedance of Physicochemical Elements of Irrigation Water Quality in Groundwater Samples. (a) pH ; (b) EC ; (c) TDS ; (d)  $\text{NO}_3^-$ -N ; (e)  $\text{Cl}^-$  ; (f)  $\text{HCO}_3^-$  ; and (g) SAR.

### Nutrient and ion concentrations

Nutrient and ion concentrations revealed complex groundwater chemical dynamics across sampling periods:

Nitrate-nitrogen ( $\text{NO}_3^-$ -N) concentrations exhibited significant seasonal fluctuation, with mean levels of  $24.06 \text{ mg}\cdot\text{L}^{-1}$  in the dry season increasing to  $32.36 \text{ mg}\cdot\text{L}^{-1}$  in the wet period (Fig. 6d). Notably, the percentage of samples exceeding FAO standards increased dramatically from 12.82% during the dry season to 69.23% during the rainy season. This substantial increase suggests intensified leaching of nitrogen compounds from agricultural soils and potential contamination from untreated domestic wastewater during periods of higher precipitation.

Chloride ( $\text{Cl}^-$ ) analysis demonstrated higher mean concentrations during the dry season ( $303.53 \text{ mg}\cdot\text{L}^{-1}$ ) compared to the rainy period ( $263.42 \text{ mg}\cdot\text{L}^{-1}$ ) (Fig. 6e). The proportion of samples surpassing recommended thresholds decreased from 23.07% in the dry season to 10.26% in the rainy season, indicating dilution effects during periods of higher rainfall.

Bicarbonate ( $\text{HCO}_3^-$ ) levels remained relatively consistent between seasons, with mean concentrations of  $442.69 \text{ mg}\cdot\text{L}^{-1}$  and  $439.53 \text{ mg}\cdot\text{L}^{-1}$  in the dry and rainy periods, respectively (Fig. 6f). The majority of samples complied with FAO standards, with only 15.38% and 7.69% of samples from dry and wet seasons, respectively, exceeding these standards.

### Sodium adsorption ratio and anthropogenic influences

Sodium Adsorption Ratio (SAR) values ranged from 3.46 to 9.5 during the dry season and narrowed to 2.73–3.67 during the wet period (Fig. 6g). While most samples adhered to FAO standards, one sample (GWS-29) deviated significantly from the recommended guidelines, highlighting localized water quality concerns potentially linked to specific land use practices or geological factors.

The analysis revealed that nitrate-nitrogen and chloride concentrations consistently exceeded quality standards across both seasons, strongly indicating significant anthropogenic interference in groundwater composition. The elevated nitrate levels, particularly during the rainy season, suggest intensive agricultural activities involving nitrogen-based fertilizers in the study area. This seasonal pattern indicates that rainfall events mobilize accumulated nitrates in the soil zone, transporting them to the underlying aquifer. Additionally, the spatial distribution of these contaminants correlates with areas of dense human settlement and agricultural intensification, further substantiating the anthropogenic origin of these pollutants.

These findings underscore the critical impact of human activities (specifically agricultural practices, wastewater disposal, and urban development) on regional groundwater chemistry. The results emphasize the urgent need for implementing comprehensive water resource management strategies, including improved agricultural practices, wastewater treatment facilities, and regular monitoring programs to safeguard groundwater quality for sustainable irrigation use.

## Spatiotemporal dynamics of groundwater chemical characteristics

The investigation unveiled intricate spatiotemporal variations in groundwater chemical parameters across the Hennaya Plain, employing advanced geospatial and interpolation techniques using QGIS software to generate comprehensive spatial mappings.

### Electrical conductivity (EC) variations

Electrical conductivity demonstrated pronounced seasonal fluctuations, revealing complex spatial patterns. During the dry period, EC values oscillated between  $1402$  and  $1850 \text{ } (\mu\text{S}\cdot\text{cm}^{-1})$  (Fig. 7a), with maximum concentrations predominantly observed in the northern and southern territories. The rainy season presented a contrasting scenario, with EC values ranging from  $1359$  to  $1643 \text{ } (\mu\text{S}\cdot\text{cm}^{-1})$  (Fig. 7b), characterized by differential spatial distributions. The observed heterogeneity in EC values suggests multifaceted influences, potentially stemming from intricate interactions between climatic conditions, geological substrata, and anthropogenic interventions. These variations underscore the dynamic nature of groundwater systems and their sensitivity to environmental and human-induced transformations.

### Sodium adsorption ratio (SAR) dynamics

Sodium Adsorption Ratio exhibited significant temporal variations, reflecting the complex ionic interactions within the groundwater system. The dry period recorded SAR values (Fig. 7c) spanning 3.45 to 9.5, dramatically transitioning to a range of 2.73 to 3.67 during the wet season (Fig. 7d). This substantial reduction suggests nuanced seasonal modifications in sodium concentration and potential ion exchange mechanisms.

The consistent moderate to high sodium content throughout the annual cycle indicates potential implications for soil structure, irrigation efficiency, and long-term agricultural sustainability.

### Sodium concentration distribution

Sodium concentrations demonstrated distinctive seasonal and geographical characteristics. During the dry period, sodium levels ranged from  $6.07$  to  $19.58 \text{ (meq}\cdot\text{L}^{-1}$ ), with notably high concentrations observed in the middle parts of the plain (Fig. 7e). The wet season presented a different pattern, with sodium values between  $4.93$  and  $6.55 \text{ (meq}\cdot\text{L}^{-1}$ ), exhibiting a geographical gradient that progressively increased from the southern to the northern regions (Fig. 7f). The spatial distribution revealed a clear concentration gradient, with sodium levels progressively increasing from the southern territories towards the northern areas. This spatial heterogeneity potentially reflects underlying geological variations, groundwater flow dynamics, and localized hydrogeochemical processes.

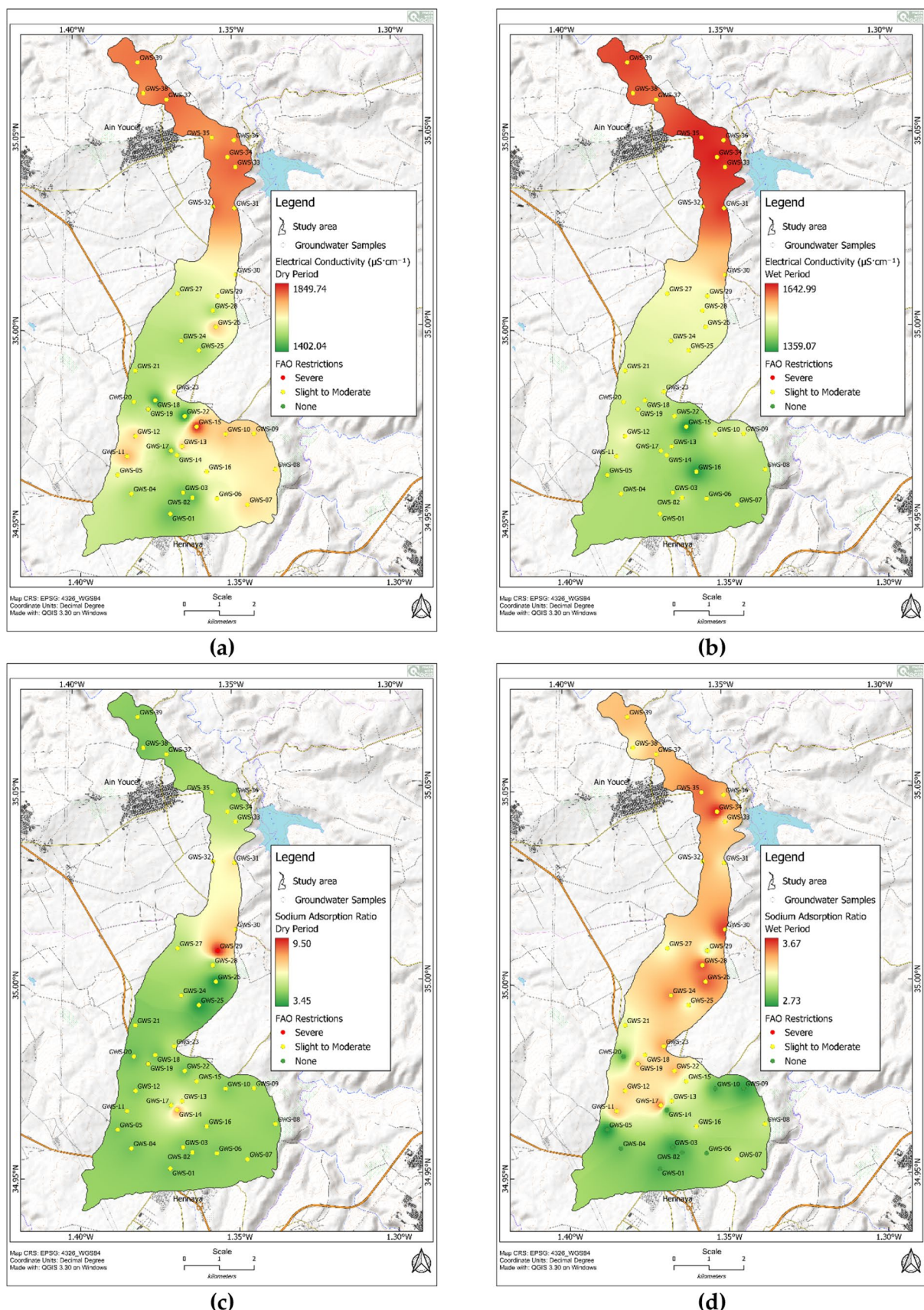


**Fig. 7.** Spatial Distribution of Irrigation Groundwater Quality Parameters: (a, b) Electrical Conductivity (EC) in Dry and Rainy Periods ; (c, d) Sodium Adsorption Ratio (SAR) in Dry and Rainy Periods ; (e, f) Sodium ( $\text{Na}^+$ ) in Dry and Rainy Periods ; (g, h) Chloride ( $\text{Cl}^-$ ) in Dry and Rainy Periods ; and (i, j) Bicarbonate ( $\text{HCO}_3^{--}$ ) in Dry and Rainy Periods. Maps were generated by QGIS 3.30.1 (<https://qgis.org>).

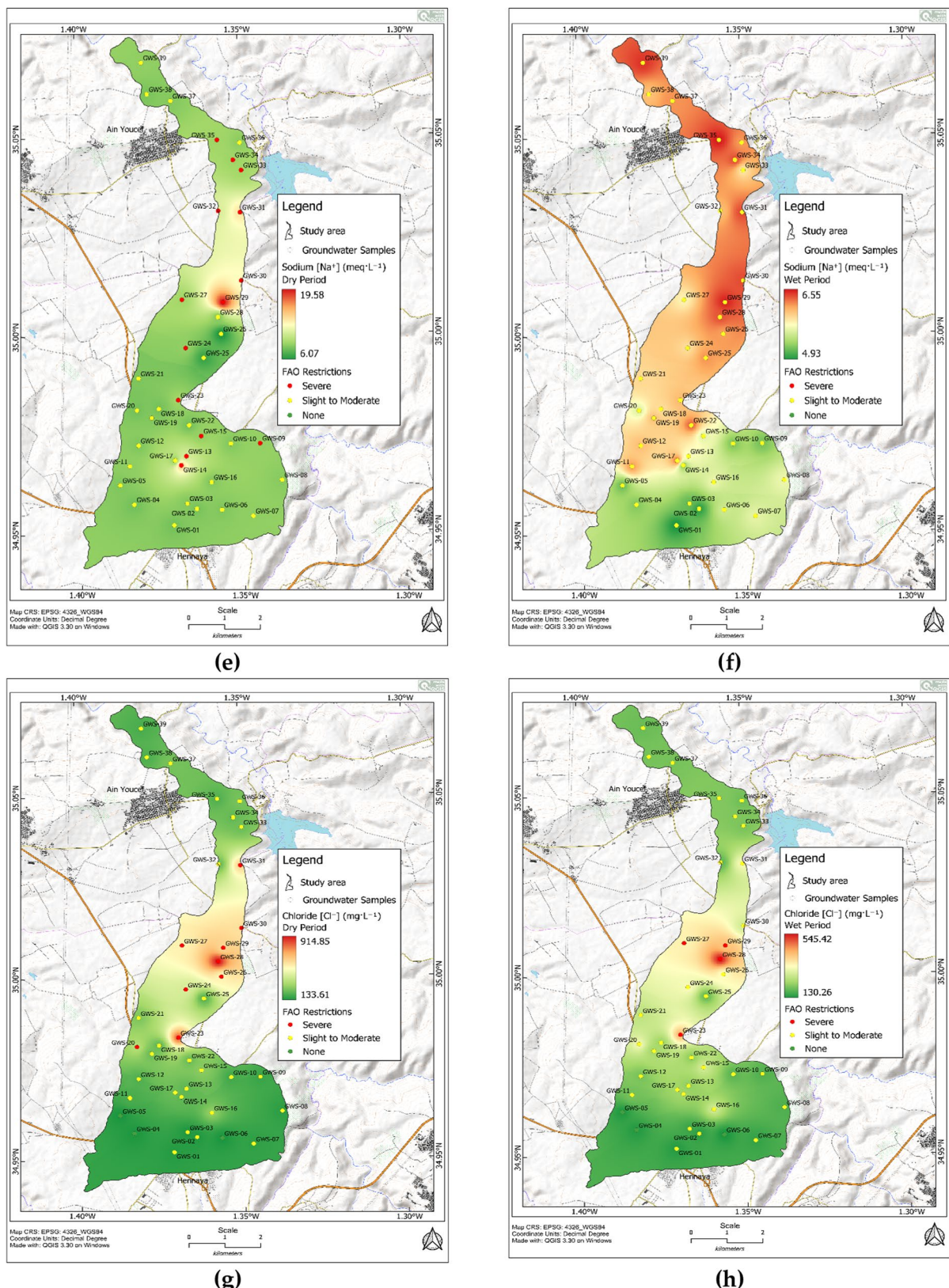


Fig. 7. (continued)

#### Chloride concentration patterns

Chloride levels displayed remarkable spatial consistency across seasonal transitions (Fig. 7g, h), with noteworthy regional variations. Concentration peaks were observed in distinct zones: 600 (mg·L<sup>-1</sup>) in the eastern region, 550

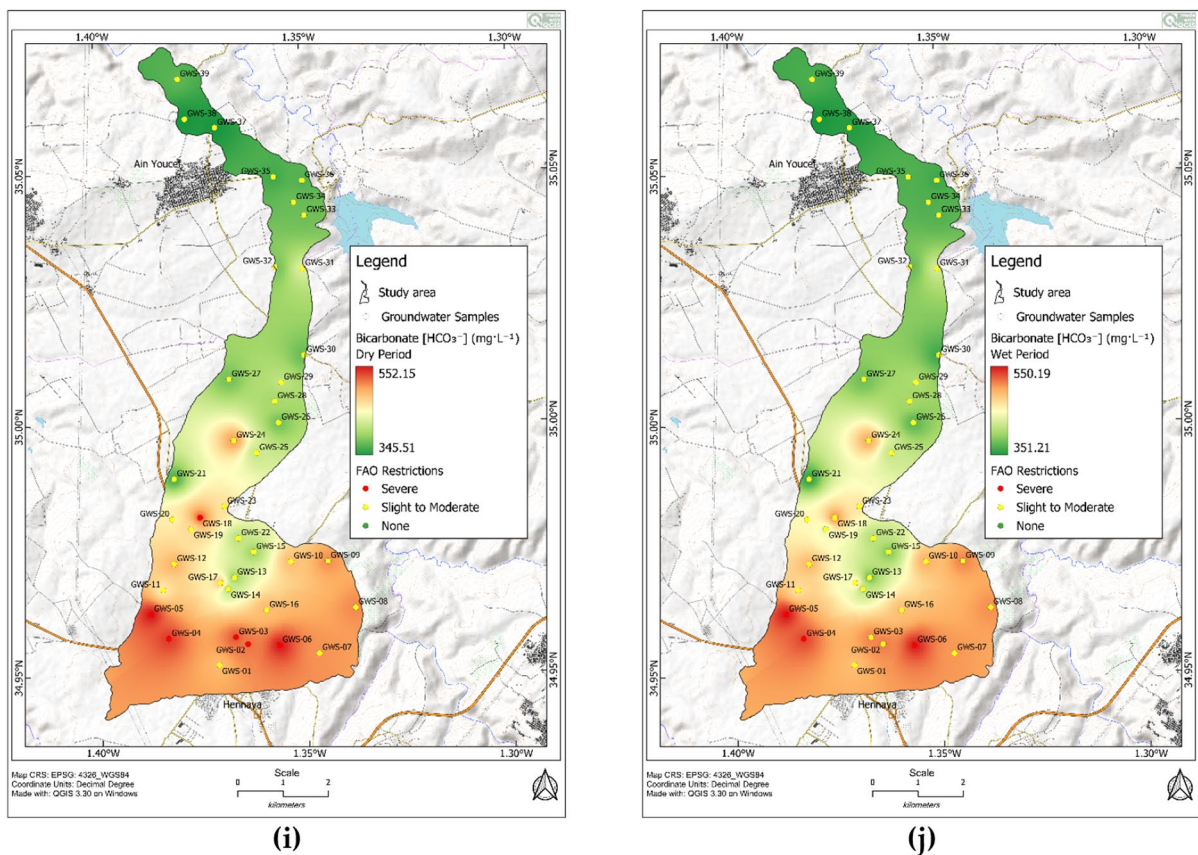


Fig. 7. (continued)

( $\text{mg}\cdot\text{L}^{-1}$ ) in the western territories, and a substantial 915 ( $\text{mg}\cdot\text{L}^{-1}$ ) in the central plain. Conversely, the northern and southern sectors demonstrated the lowest chloride concentrations. The significant chloride concentration variations may strongly correlate be with intensive agricultural practices, particularly the extensive application of chloride-rich fertilizers. These findings underscore the profound anthropogenic influences on groundwater chemical composition.

#### Bicarbonate distribution characteristics

Bicarbonate distribution presented a unique spatial pattern divergent from other chemical constituents. Consistent across both dry and wet seasons, bicarbonate contents ranged globally between  $345.5\text{ mg}\cdot\text{L}^{-1}$  and  $552.15\text{ (mg}\cdot\text{L}^{-1})$  (Fig. 7i, j). Elevated bicarbonate levels were predominantly concentrated in southern zones adjacent to Hennaya city, attributed to the substantial geological contribution from Jurassic carbonate formations of the Tlemcen Mountains. In contrast, northern and central aquifer regions, characterized by coarse alluvial deposits, exhibited markedly lower bicarbonate concentrations.

#### Irrigation water quality index (IWQI) analysis

The Irrigation Water Quality Index (IWQI) assessment revealed significant seasonal variations in groundwater suitability for irrigation purposes. During the dry period, IWQI values ranged from 29.25 to 65.35 (Fig. 8a), with a complex distribution of water quality classifications. Specifically, 76.92% of groundwater samples demonstrated moderate pollution, 15.38% exhibited high pollution, and 7.69% were classified as severely polluted. These findings suggest that during the dry season, the groundwater is marginally suitable for irrigation, primarily appropriate for salt-tolerant plants in highly permeable soils<sup>26</sup>. The central areas of the plain, characterized by intensive agricultural activities, showed the most pronounced pollution concentrations. In contrast, the rainy season demonstrated a notable improvement in water quality (Fig. 8b). All samples were classified as moderately polluted, indicating enhanced suitability for irrigating medium salt-tolerant plants in soils of moderate permeability<sup>26</sup>. This dramatic shift underscores the substantial impact of seasonal factors on groundwater characteristics. Geospatial analysis using GIS interpolation further validated these observations, revealing distinct spatial patterns of water quality variations. The dry season maps highlighted localized severe pollution zones (Fig. 8c), while the wet season maps showed a more uniform and improved water quality distribution across the study area (Fig. 8d). The research emphasizes the critical relationship between seasonal dynamics and groundwater quality. The significant variations observed suggest that agricultural practices, precipitation patterns, and hydrological processes interact complexly to influence irrigation water suitability. These findings highlight the necessity for adaptive water management strategies, particularly during dry periods

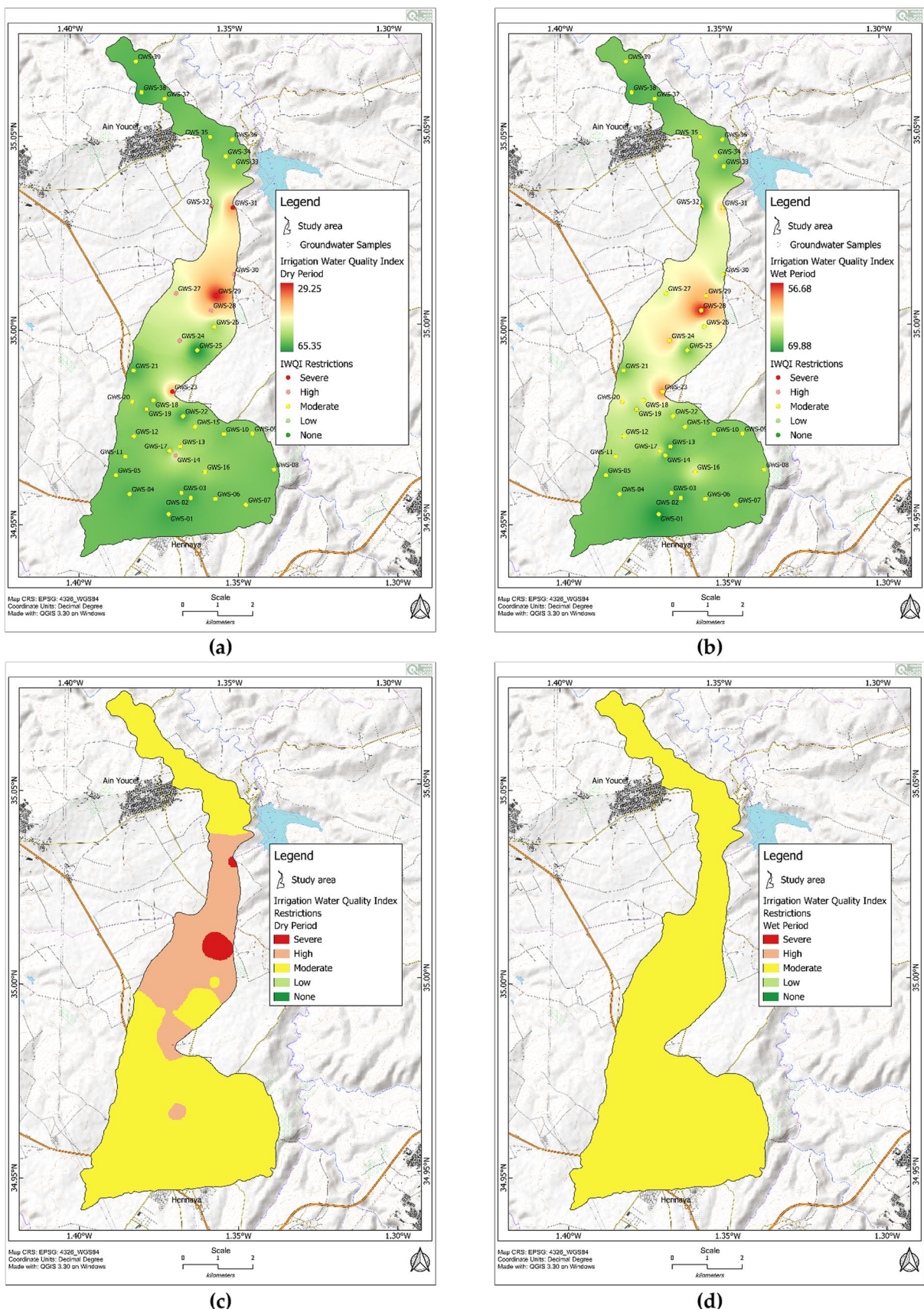


**Fig. 8.** (a, b) Spatial Distribution of Irrigation Water Quality According to IWQI in the Dry and Wet Seasons; (c, d) Categories of Irrigation Groundwater Quality based on IWQI Restrictions in the Dry and Rainy Periods. Maps were generated by QGIS 3.30.1 (<https://qgis.org>).

when groundwater quality is most compromised. Despite the improvement during wet periods, the persistent moderate pollution level underscores ongoing environmental challenges.

### Nitrate-Nitrogen ( $\text{NO}_3^-$ -N) contamination dynamics

The groundwater analysis revealed complex seasonal variations in nitrate-nitrogen ( $\text{NO}_3^-$ -N) concentrations, providing critical insights into regional environmental and agricultural dynamics. During the dry period, nitrate levels ranged from 12.79 to 45.53 ( $\text{mg L}^{-1}$ ) (Fig. 9a), indicating moderate to severe contamination potential, with the most pronounced pollution concentrated in the central, agriculturally intensive areas of the plain (Fig. 9c). The wet season demonstrated a notable transformation in spatial distribution and concentration patterns. Nitrate-nitrogen levels increased, fluctuating between 22.14 and 49.05 ( $\text{mg L}^{-1}$ ) (Fig. 9b), with contamination areas expanding to encompass larger portions of the study region (Fig. 9d). This expansion suggests multiple contamination sources and complex hydrological interactions.

Land-use analysis (Fig. 1b) reveals strong spatial correlations between agricultural intensity and nitrate contamination patterns. The central plain, characterized by intensive crop cultivation covering approximately 75% of the study area, exhibits the highest nitrate concentrations consistently across both seasons. Agricultural land-use mapping demonstrates that areas with continuous cropping systems and high fertilizer application rates ( $> 200 \text{ kg N/ha annually}$ ) correspond directly to  $\text{NO}_3^-$ -N hotspots exceeding  $40 \text{ mg L}^{-1}$ . Peripheral zones with extensive agriculture and lower fertilization intensity show correspondingly reduced nitrate levels (15–25  $\text{mg L}^{-1}$ ), establishing a clear contamination gradient from intensive to extensive agricultural areas.

The observed increase in nitrate concentrations during the wet season likely results from precipitation-induced mobilization mechanisms. Increased rainfall appears to facilitate the loading of organic pollutants from surface layers into the aquifer, a phenomenon consistent with established hydrogeological understanding of contaminant transport<sup>71–73</sup>. The observed increase in nitrate concentrations during the wet season likely results from precipitation-induced mobilization mechanisms. Increased rainfall appears to facilitate the loading of organic pollutants from surface layers into the aquifer, a phenomenon consistent with established hydrogeological understanding of contaminant transport<sup>71–73</sup>. Enhanced soil leaching during wet periods promotes the vertical migration of nitrogen compounds through the vadose zone into the saturated aquifer.

Temporal analysis of contamination sources reveals seasonal shifts in nitrate mobilization mechanisms. During dry periods, nitrate contamination primarily reflects accumulated fertilizer residues and soil organic nitrogen mineralization under water-limited conditions. The wet season introduces enhanced leaching of recently applied fertilizers, decomposing organic matter, and mobilization of previously immobilized nitrogen from soil matrices. This seasonal dynamic explains the observed 25–30% increase in average nitrate concentrations during wet periods.

Geospatial analysis using interpolation techniques highlighted the dynamic nature of nitrate distribution. Dry season maps revealed localized pollution hotspots, while wet season representations showed a more widespread contamination pattern, underscoring the significant impact of seasonal environmental conditions on groundwater chemistry. These findings emphasize the need for comprehensive monitoring and targeted interventions to mitigate agricultural and environmental risks associated with nitrate contamination. The research suggests that seasonal variations play a crucial role in nitrate mobility and distribution, highlighting the importance of adaptive management strategies in groundwater protection.

### Integration of irrigation water quality index (IWQI) with Nitrate-Nitrogen distribution

The integration of the Irrigation Water Quality Index (IWQI) with nitrate-nitrogen ( $\text{NO}_3^-$ -N) distribution represents a novel approach to comprehensively evaluating irrigation water chemistry in this agriculturally intensive region. The research unveils a complex landscape of groundwater quality that transcends traditional single-parameter assessments, revealing intricate spatial and temporal dynamics that have significant implications for agricultural sustainability. The results demonstrate a nuanced pattern of water quality variation across different seasonal contexts. During the dry season, the water quality categories exhibit a heterogeneous distribution, with poor quality dominating the central sectors and moderate quality characterizing the northern and southern regions (Fig. 10a). This spatial variability suggests complex interactions between hydrogeological conditions and anthropogenic influences that shape groundwater chemical composition. The wet season introduces a more pronounced transformation in water quality characteristics. A notable deterioration emerges, with poor quality water predominantly occupying most of the alluvial aquifer system (Fig. 10b). This seasonal shift highlights the dynamic nature of groundwater chemistry, demonstrating how hydrological cycles and environmental factors can rapidly alter water quality parameters. The IWQI analysis revealed critical indicators of groundwater quality, including significant challenges such as high salinity levels, elevated alkalinity, and pronounced groundwater toxicity. These findings point to potential severe consequences for soil health and agricultural productivity. The chemical composition suggests a complex interplay between natural hydrogeological processes and human-induced environmental modifications<sup>72</sup>. Hydrological processes significantly influence groundwater chemistry dynamics. During dry periods, limited aquifer replenishment concentrates dissolved salts and carbonates, creating a distinct chemical signature. Conversely, the wet season introduces increased aquifer recharge, temporarily diluting these chemical concentrations and creating a more complex hydrochemical environment. Nitrate pollution emerged as a critical component of the integrated assessment. Agricultural practices, particularly the intensive use of nitrogen-rich fertilizers, appear to be a primary driver of groundwater  $\text{NO}_3^-$ -N contamination. The research demonstrates how soil leaching processes, especially during high precipitation periods, facilitate the rapid transport of nitrogen compounds through the aquifer system. The wet season amplifies the potential for nitrate mobilization, with increased precipitation rates enhancing soil leaching mechanisms. This process promotes the vertical and lateral migration of nitrogen compounds, creating a dynamic system of nutrient transport that extends beyond traditional understanding of groundwater chemistry. The findings underscore the

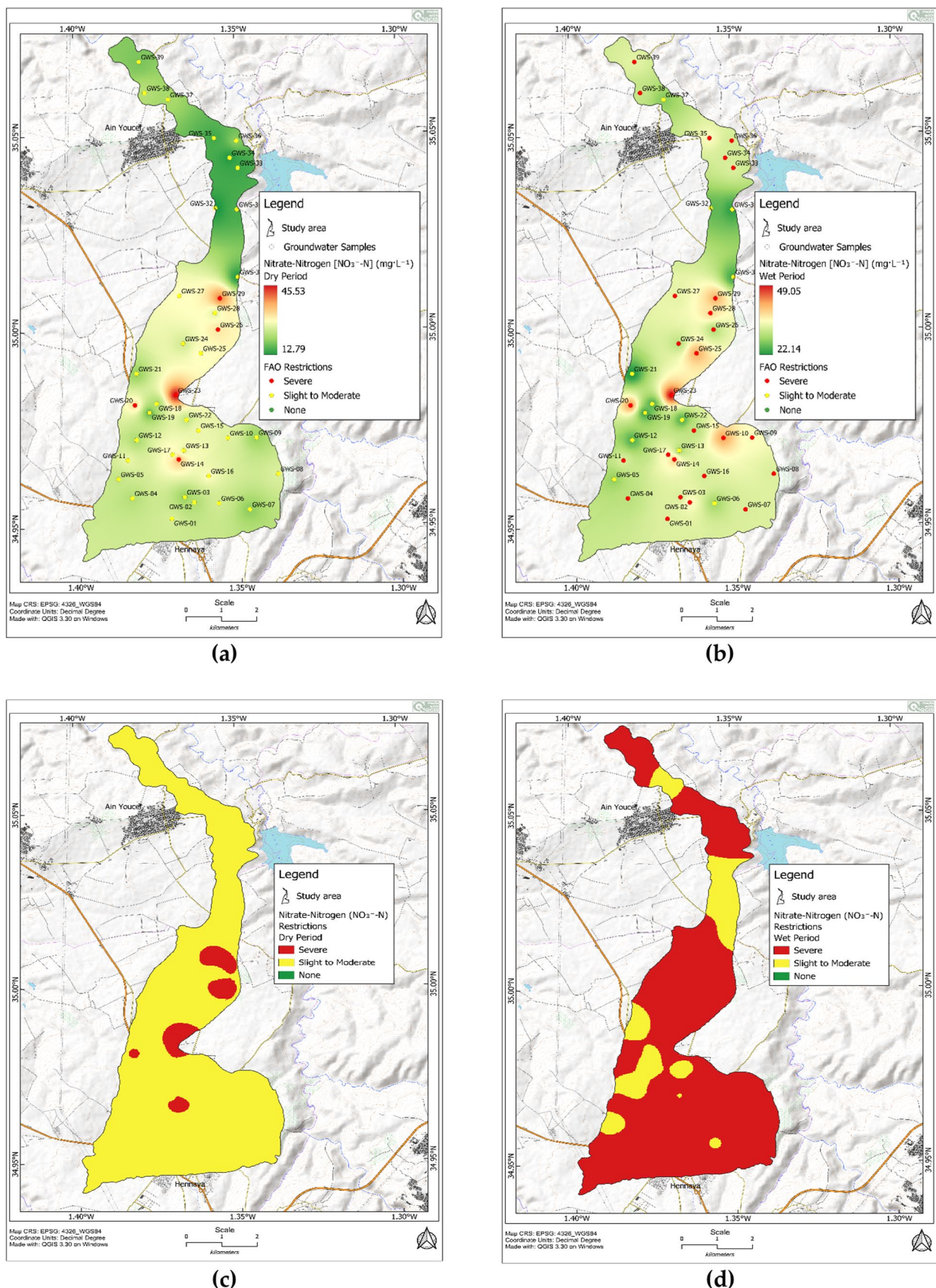


**Fig. 9.** (a, b) Spatial Distribution of Irrigation Water Quality According to  $\text{NO}_3^-\text{-N}$  in the Dry and Wet Seasons ; (c, d) Categories of Irrigation Groundwater Quality based on FAO Standards in the Dry and Rainy Periods. Maps were generated by QGIS 3.30.1 (<https://qgis.org>).

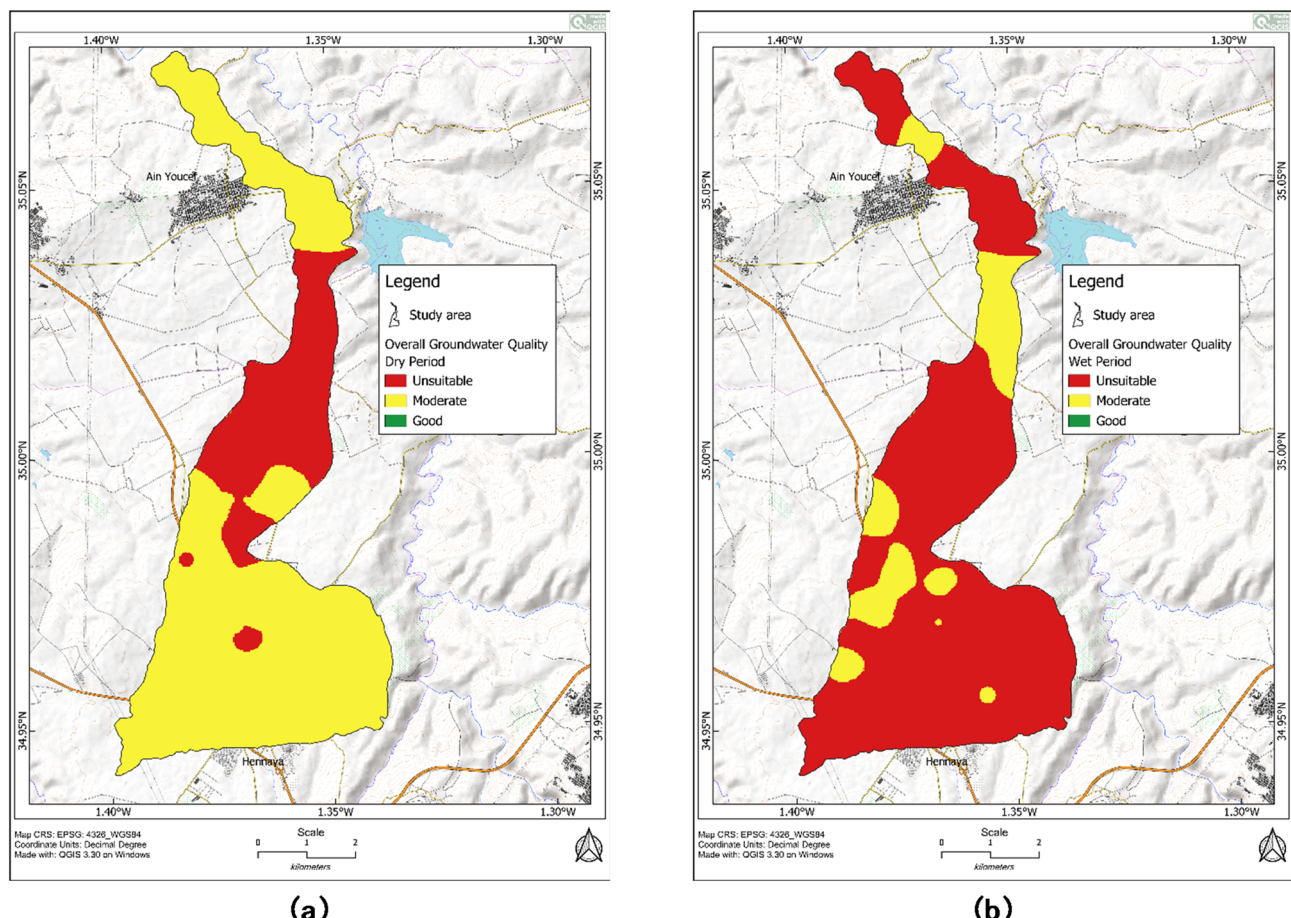


**Fig. 10.** Overall Suitability of Groundwater for Irrigation (a) Dry Season ; (b) wet Season. Maps were generated by QGIS 3.30.1 (<https://qgis.org>).

critical need for targeted agricultural management strategies that can mitigate nutrient runoff and groundwater contamination.

This integrated approach provides unprecedented insights into the complex dynamics of irrigation water resources. By simultaneously examining multiple water quality parameters and their seasonal variations, the study offers a more comprehensive understanding of groundwater systems than traditional single-parameter assessments. The observed water quality deterioration, particularly during the wet season, presents significant challenges for sustainable agricultural practices. The research highlights urgent needs for refined agricultural strategies, including more precise fertilization techniques, enhanced soil management approaches, and comprehensive groundwater monitoring programs. These findings have broader implications for regional agricultural sustainability, water resource management, and environmental conservation.

## Discussion

The present study provides a comprehensive and multidimensional examination of groundwater quality in the region, revealing complex seasonal dynamics of nitrate-nitrogen ( $\text{NO}_3^-$ -N) concentrations and irrigation water quality index (IWQI). The findings of this research elucidate the intricate interaction between agricultural practices, precipitation regimes, and groundwater contamination, offering critical insights into the environmental challenges facing the study area. Comprehensive source attribution analysis reveals multiple pathways contributing to groundwater nitrate contamination in the Hennaya Plain. Land-use mapping demonstrates strong spatial correlations between agricultural intensity and contamination patterns, with the central agricultural zone covering approximately 75% of the study area exhibiting consistently highest nitrate concentrations across both seasons. Areas characterized by intensive crop cultivation and fertilizer application rates exceeding 200 kg N/ha annually correspond directly to nitrate hotspots surpassing  $40 \text{ mg L}^{-1}$ , while peripheral zones with extensive agriculture show reduced levels ( $15\text{--}25 \text{ mg L}^{-1}$ ), establishing a clear contamination gradient. Seasonal variations in groundwater quality demonstrated significant and nuanced dynamics. Nitrate concentrations showed an atypical pattern, increasing during the wet season, contrary to the dilution effect observed for other water quality parameters. This phenomenon can be attributed to enhanced leaching of organic contaminants during rainy periods, with precipitation facilitating pollutant mobilization from surface soils into the aquifer system. Enhanced soil leaching during wet periods promotes vertical migration

of nitrogen compounds through the vadose zone, with average concentration expanding from 24.06 mg.L<sup>-1</sup> of the study area during dry periods to 32.36 mg.L<sup>-1</sup> during wet seasons. This seasonal dynamic explains the observed 34.5% increase in average nitrate concentrations during wet periods, reflecting enhanced mobilization of recently applied fertilizers and decomposing organic matter. These elevated nitrate levels pose significant public health risks, as consumption of water exceeding the WHO guideline value of 50 mg.L<sup>-1</sup> NO<sub>3</sub><sup>-</sup> (or 11.3 mg.L<sup>-1</sup> NO<sub>3</sub><sup>-</sup>-N) has been associated with methemoglobinemia in infants (“blue baby syndrome”) and potential links to certain cancers and reproductive issues in adults<sup>10,11</sup>. Additionally, excessive nitrates in agricultural water can disrupt aquatic ecosystems through eutrophication, causing algal blooms, oxygen depletion, and biodiversity loss in connected surface water bodies<sup>35</sup>. Principal Component Analysis demonstrated a significant shift in NO<sub>3</sub><sup>-</sup>-N behavior between seasons, transitioning from association with anthropogenic factors (F2 axis) in the dry season to integration with mineralization processes (F1 axis) in the wet season, explaining the paradoxical increase in nitrate concentrations despite dilution of other parameters. Hierarchical Cluster Analysis confirmed this pattern, showing NO<sub>3</sub><sup>-</sup>-N clustering with agricultural indicators (Ca<sup>2+</sup>, Mg<sup>2+</sup>) during the dry season but forming more complex associations during the wet season at lower dissimilarity thresholds (1.2 versus 1.6). These statistical findings align with spatial observations showing severe pollution concentrated in agricultural zones during the dry season and expanding across a wider area during the wet season, consistent with research from similar Mediterranean semi-arid regions<sup>41-44</sup>. The Irrigation Water Quality Index (IWQI) results revealed a remarkable seasonal transformation. During the dry season, groundwater quality ranged from moderate to severe pollution, while the wet season showed a significant improvement with all samples classified as moderately polluted. This shift underscores the complex dilution mechanisms of rainwater on groundwater pollutants. The severe pollution classifications are particularly concerning as they indicate water with potentially harmful levels of salinity, sodium hazard, and specific ion toxicity that can damage crops, reduce agricultural productivity, and eventually lead to soil degradation through salinization; an often irreversible process that threatens long-term food security in the region<sup>26</sup>. Spatial analysis provided critical insights into the distribution of groundwater contamination. During the dry season, severe pollution was concentrated in the central, agriculturally intensive regions of the plain. The wet season witnessed an expansion of contamination, with nitrate pollution spreading across a larger area. This pattern underscores the pivotal role of precipitation in transporting and redistributing organic pollutants from the external environment into the aquifer. The seasonal fluctuations in groundwater pollution sources were particularly noteworthy. While most elements showed reduced concentrations during the wet season, nitrate levels demonstrated an inverse trend, suggesting multiple contamination pathways and the need for nuanced groundwater management approaches. A critical observation from this study is the apparent contradiction between improved IWQI classifications (from severe to moderate pollution) and simultaneously increased nitrate contamination (34.5% increase) during the wet season. This paradox highlights important limitations in the sensitivity of composite water quality indices to specific health-critical parameters. While the IWQI showed overall improvement due to dilution effects on salinity parameters (EC, SAR, Na<sup>+</sup>, Cl<sup>-</sup>), the index’s weighting system may inadequately reflect the heightened risks posed by elevated nitrate-nitrogen concentrations. The IWQI’s composite nature, which averages multiple parameters, can mask the significance of individual contaminants of high toxicological concern such as NO<sub>3</sub><sup>-</sup>-N. This finding suggests that relying solely on composite indices may provide misleading assessments of water safety, particularly regarding parameters with stringent health guidelines. The WHO guideline value of 11.3 mg.L<sup>-1</sup> NO<sub>3</sub><sup>-</sup>-N was exceeded in numerous samples during the wet season despite improved IWQI scores, indicating potential health risks that the composite index failed to adequately highlight. This discrepancy underscores the need for complementary assessment approaches that give appropriate weight to health-critical parameters alongside composite indices, ensuring that improvements in general water quality metrics do not obscure emerging contamination threats. The observed seasonal groundwater contamination dynamics in the Hennaya Plain resonate with critical research from other Mediterranean semi-arid agricultural landscapes, where contextualization of these findings through comparative research reveals significant parallels with regional studies. Khouli et al.<sup>41</sup> in similar agricultural regions of Mitidja plain revealed comparable patterns of nitrate contamination, particularly highlighting the role of intensive agricultural practices in groundwater quality degradation during rainy periods. Specifically, Zufiaurre et al.<sup>42</sup> in their research on the shallow aquifers in the northeastern regions of Spain demonstrated analogous seasonal variations in groundwater chemistry, with wet seasons facilitating enhanced nutrient mobilization—a phenomenon closely mirroring our findings. Bourmada et al.<sup>43</sup> investigating groundwater systems in Souk Ahras’s semi-arid regions (Algeria), also reported similar spatial patterns of contamination concentration in agricultural zones, further validating our observations of localized pollution hotspots. The pronounced seasonal transformations in water quality, ranging from moderate to severe pollution, align with research by Tlili-Zrelli et al.<sup>44</sup> in Tunisian agricultural plains, which emphasized the critical interaction between agricultural intensification and groundwater vulnerability in Mediterranean ecosystems and its relationship to seasonal variations. Based on these findings, several critical recommendations emerge for sustainable water resource management. Crop selection strategies should prioritize salt-tolerant and nitrate-resistant varieties, including sorghum, barley, millet, and specific citrus varieties that can thrive in challenging environmental conditions<sup>4,75</sup>. Implementing precision agriculture techniques, developing comprehensive monitoring programs, and creating robust regulatory frameworks are essential for mitigating groundwater degradation. The study makes several significant scientific contributions to understanding groundwater dynamics, including:

1. A detailed characterization of seasonal variations in nitrate contamination;
2. Comprehensive mapping of irrigation water quality across dry and wet seasons;
3. Identification of key factors influencing groundwater pollution in agricultural landscapes.

Several methodological limitations should be acknowledged. The research was conducted over a limited time frame, and long-term monitoring would provide more definitive insights into temporal patterns and cyclical variations in groundwater quality. Future studies should incorporate multi-year monitoring programs to better characterize long-term trends and distinguish between seasonal fluctuations and progressive changes in aquifer conditions. The study focused on a specific geographical region, and results may not be directly generalizable to all agricultural landscapes. Expanding research to diverse agricultural settings with varying crops, management practices, and hydrogeological conditions would enhance the generalizability of findings and allow for comparative analyses across different contexts. While the IWQI and nitrate analysis provide valuable insights, additional parameters such as pesticide residues, heavy metals, and microbiological indicators could offer a more comprehensive assessment of groundwater quality. Future research integrating these parameters would provide a more holistic understanding of contamination dynamics.

To mitigate ongoing groundwater degradation, the study emphasizes the critical need to:

1. Control the indiscriminate use of agricultural fertilizers and pesticides, with future research focusing on optimizing application rates based on crop-specific needs and local hydrogeological vulnerability factors;
2. Implement targeted management strategies accounting for seasonal variations, supported by future studies that develop predictive models to anticipate seasonal changes in groundwater vulnerability;
3. Develop more sophisticated monitoring systems to dynamically track groundwater quality, with future research exploring cost-effective sensor networks and remote sensing techniques that could provide real-time data on groundwater conditions.

The research underscores the complex nature of groundwater contamination in agricultural landscapes. The pronounced seasonal variations in nitrate content and irrigation water quality demand adaptive management approaches capable of responding to dynamic environmental conditions. Future interdisciplinary research combining hydrogeology, agricultural science, and policy analysis could address these gaps by developing integrated decision support systems that balance agricultural productivity with groundwater protection.

## Conclusion

The groundwater quality assessment of the Hennaya Plain aquifer provides a comprehensive investigation into the complex dynamics of water contamination, revealing critical insights into the environmental challenges faced by agricultural regions. The research employed a novel methodological approach, integrating the Irrigation Water Quality Index (IWQI) with detailed  $\text{NO}_3^-$ -N content analysis to evaluate spatiotemporal variations in groundwater quality during dry and wet seasons. Key findings demonstrated significant seasonal variations in groundwater chemistry, with average  $\text{NO}_3^-$ -N concentrations ranging from 24.06 ( $\text{mg.L}^{-1}$ ) in the dry period to 32.36 ( $\text{mg.L}^{-1}$ ) in the wet period, and  $\text{Cl}^-$  concentrations shifting from 303.53 to 263.42 ( $\text{mg.L}^{-1}$ ). Critically, 12.82% and 69.23% of samples exceeded FAO standards for  $\text{NO}_3^-$ -N, while 23.07% and 10.26% of samples surpassed chloride limits, indicating severe water quality impairment driven by human agricultural practices. The scientific contribution of this study lies in its comprehensive spatial and temporal analysis of groundwater contamination. The research uniquely mapped chemical element distributions, revealing highest concentrations of  $\text{Cl}^-$ ,  $\text{Na}^+$ , and  $\text{NO}_3^-$ -N in the central plain's agricultural areas. This precise identification of pollution sources demonstrates the direct relationship between intensive agricultural activities and groundwater degradation, a critical advancement in understanding environmental-agricultural interactions. Temporal trend analysis revealed a complex contamination pattern, with the Irrigation Water Quality Index (IWQI) ranging from 29.25 to 65.35 in the dry period and 56.85 to 69.88 in the rainy period. The dry season showed more severe water quality classifications, suitable only for highly salt-tolerant plants in high-permeability soils, while the wet season exhibited moderate pollution levels appropriate for plants with medium salt tolerance. Notably, the study uncovered a unique nitrate contamination dynamic, with higher concentrations during the wet season. This counterintuitive finding highlights the role of precipitation in transporting organic pollutants, explaining how rainfall contributes to the distribution of contaminants from external environments into the aquifer. The research suggests that selecting agricultural crops with inherent resilience to saline and nitrate-rich environments is crucial. The mean implications point towards identifying and cultivating plant varieties that demonstrate superior adaptation to challenging water and soil conditions. The central recommendation centers on integrating advanced agricultural methodologies, systematic monitoring approaches, and regulatory mechanisms to address and mitigate groundwater contamination and degradation. Future interventions must focus on controlling agricultural fertilizer and pesticide use, implementing preventive measures to address salinization and soil structure degradation. Recommended strategies include developing targeted farmer training programs with mandatory certification for fertilizer application, particularly for the farmers in the central contamination zone where  $\text{NO}_3^-$ -N concentrations exceeded 45  $\text{mg.L}^{-1}$ . Establishing 50-meter vegetated buffer zones between agricultural areas and water recharge zones, planted with nitrogen-fixing leguminous cover crops, should be prioritized around wells exceeding FAO nitrate standards. Implementing precision agriculture with maximum nitrogen application limits of 150 kg N/ha in high-risk zones, and installing drip irrigation systems to replace flood irrigation in the current agricultural areas can reduce water usage by 30–40% while minimizing nutrient leaching. Seasonal monitoring frameworks should deploy 20–25 monitoring wells with quarterly sampling during dry periods and monthly sampling during wet seasons, focusing on the central agricultural zone. Research directions should prioritize long-term ecological risk assessments, developing predictive groundwater quality models, exploring bioremediation techniques, and investigating the potential health impacts of prolonged groundwater contamination. Additionally, studies should focus on developing machine learning approaches for contamination prediction, and investigating indigenous plant species for phytoremediation applications. The methodology and insights presented offer a foundational approach to water resource management that can be

applied to similar agricultural regions facing environmental challenges. Ultimately, this research serves as a critical scientific contribution and a call to action for researchers, policymakers, and local communities. By providing a detailed understanding of groundwater contamination dynamics, the study offers a scientific basis for developing targeted interventions that balance agricultural productivity with environmental conservation, emphasizing the urgent need for integrated strategies to protect this vital resource.

## Data availability

The datasets used and/or analyzed during the current study are available from the corresponding author upon reasonable request.

Received: 8 January 2025; Accepted: 11 June 2025

Published online: 02 July 2025

## References

1. Golchin, I. & Azhdary Moghaddam, M. Hydro-geochemical characteristics and groundwater quality assessment in Iranshahr plain aquifer, Iran. *Environ. Earth Sci.* **75**, 1–14. <https://doi.org/10.1007/s12665-015-5077-0> (2016).
2. Zhang, Q., Wang, H., Wang, Y., Yang, M. & Zhu, L. Groundwater quality assessment and pollution source apportionment in an intensely exploited region of Northern China. *Environ. Sci. Pollut. Res.* **24**, 16639–16650. <https://doi.org/10.1007/s11356-017-9114-2> (2017).
3. Li, Y. et al. Investigation of quality and pollution characteristics of groundwater in the Hutuo river alluvial plain, North China plain. *Environ. Earth Sci.* **75**, 1–10. <https://doi.org/10.1007/s12665-016-5366-2> (2016).
4. Zhang, Q., Wang, H. & Wang, L. Tracing nitrate pollution sources and transformations in the over-exploited groundwater region of North China using stable isotopes. *J. Contam. Hydrol.* **218**, 1–9. <https://doi.org/10.1016/j.jconhyd.2018.06.001> (2018).
5. Edmunds, W. et al. Groundwater evolution in the continental intercalaire aquifer of Southern Algeria and tunisia: Trace element and isotopic indicators. *Appl. Geochem.* **18**, 805–822. [https://doi.org/10.1016/S0883-2927\(02\)00189-0](https://doi.org/10.1016/S0883-2927(02)00189-0) (2003).
6. Li, P., Wu, J. & Qian, H. Assessment of groundwater quality for irrigation purposes and identification of hydrogeochemical evolution mechanisms in Pengyang county, China. *Environ. Earth Sci.* **69**, 2211–2225. <https://doi.org/10.1007/s12665-012-2049-5> (2013).
7. Ayers, R. & Westcot, D. *Water Quality for Agriculture*. FAO Irrigation and Drainage Paper 29, rev. 1. Food and Agriculture Organization of the United Nations, Rome. 174 p.; Available online: (1985). <https://www.fao.org/3/t0234e/t0234e00.htm> (accessed on 15 October 2024).
8. Torres-Martínez, J. A., Mora, A., Knappett, P. S. K., Ornelas-Soto, N. & Mahlknecht, J. Tracking nitrate and sulfate sources in groundwater of an urbanized Valley using a multi-tracer approach combined with a bayesian isotope mixing model. *Water Res.* **182**, 115962. <https://doi.org/10.1016/j.watres.2020.115962> (2020).
9. Pastén-Zapata, E., Ledesma-Ruiz, R., Harter, T., Ramírez, A. I. & Mahlknecht, J. Assessment of sources and fate of nitrate in shallow groundwater of an agricultural area by using a multi-tracer approach. *Sci. Total Environ.* **470–471**, 855–864. <https://doi.org/10.1016/j.scitotenv.2013.10.043> (2014).
10. Rahman, A., Mondal, N. C. & Tiwari, K. K. Anthropogenic nitrate in groundwater and its health risks in the view of background concentration in a semi arid area of rajasthan, India. *Sci. Rep.* **11**, 9279. <https://doi.org/10.1038/s41598-021-88600-1> (2021).
11. Chen, J., Wu, H. & Qian, H. Assessing nitrate and fluoride contaminants in drinking water and their health risk of rural residents living in a semiarid region of Northwest China. *Expo Health.* **9**, 183–195. <https://doi.org/10.1007/s12403-016-0231-9> (2017).
12. Jia, H. et al. Alterations to groundwater chemistry due to modern water transfer for irrigation over decades. *Sci. Total Environ.* **717**, 137170. <https://doi.org/10.1016/j.scitotenv.2020.137170> (2020).
13. Khajuria, A. & Kanae, S. Potential and use of nitrate in agricultural purposes. *J. Water Resour. Prot.* **5**, 529–533. <https://doi.org/10.4236/jwarp.2013.55053> (2013).
14. Ahada, C. P. S. & Suthar, S. Groundwater nitrate contamination and associated human health risk assessment in Southern districts of punjab, India. *Environ. Sci. Pollut. Res.* **25**, 25336–25347. <https://doi.org/10.1007/s11356-018-2581-2> (2018).
15. Mahvi, A. H., Nouri, J., Babaei, A. A. & Nabizadeh, R. Agricultural activities impact on groundwater nitrate pollution. *Int. J. Environ. Sci. Technol.* **2**, 41–47. <https://doi.org/10.1007/BF03325856> (2005).
16. EPA. National Recommended Water Quality Criteria; United States Environmental Protection Agency. Office of Water, Office of Science and Technology: Washington, DC, USA, (2009).
17. Lwimbo, Z. D., Komakech, H. C. & Muzuka, A. N. Impacts of emerging agricultural practices on groundwater quality in Kahe catchment, Tanzania. *Water* **11**, 2263. <https://doi.org/10.3390/w11112263> (2019).
18. Arumugam, K. & Elangovan, K. Hydrochemical characteristics and groundwater quality assessment in Tirupur region, Coimbatore district, Tamil nadu, India. *Environ. Geol.* **58**, 1509–1520. <https://doi.org/10.1007/s00254-008-1652-y> (2009).
19. Vrba, J. The impact of aquifer intensive use on groundwater quality. In *Intensive Use of Groundwater. Challenges and Opportunities*; International Association of Hydrogeologists (IAH): Prague, The Czech Republic, 113–132, (2003).
20. Wang, Y., Li, R., Wu, X. & Yan, Y. Evaluation of groundwater quality for drinking and irrigation purposes using GIS-Based IWQI, EWQI and HHR model. *Water* **15**, 2233. <https://doi.org/10.3390/w15122233> (2023).
21. Mukherjee, I., Singh, U. K. & Chakma, S. Evaluation of groundwater quality for irrigation water supply using multi-criteria decision-making techniques and GIS in an agroeconomic tract of lower Ganga basin, India. *J. Environ. Manage.* **309**, 114691. <https://doi.org/10.1016/j.jenvman.2022.114691> (2022).
22. Kopittke, P. M., So, H. B. & Menzies, N. W. Effect of ionic strength and clay mineralogy on Na–Ca exchange and the SAR–ESP relationship. *Eur. J. Soil. Sci.* **57**, 626–633. <https://doi.org/10.1111/j.1365-2389.2005.00753.x> (2006).
23. Saleh, A., Al-Ruwaih, F. & Shehata, M. Hydrogeochemical processes operating within the main aquifers of Kuwait. *J. Arid Environ.* **42**, 195–209. <https://doi.org/10.1006/jare.1999.0511> (1999).
24. Wang, L., Long, F., Liao, W. & Liu, H. Prediction of anaerobic digestion performance and identification of critical operational parameters using machine learning algorithms. *Bioresour. Technol.* **298**, 122495. <https://doi.org/10.1016/j.biortech.2019.122495> (2020).
25. Paliwal, K. V. & Heine, R. W. Irrigation with saline water. *Q. Rev. Biol.* **4**, 198 (1972).
26. Meireles, A. C. M., Andrade, E. M., Chaves, L. C. G., Frischkorn, H. & Crisostomo L. A. A new proposal of the classification of irrigation water. *Revista Ciéncia Agronómica* **41**, 349–357. <https://doi.org/10.1590/S1806-6690201000300005> (2010).
27. Alves, T. C., Jenske, G., Cardozo, A. & Pinheiro, A. A new integrated water quality index (IWQI) and your application with emergent pollutants in the Atlantic forest biome basin in Southern Brazil. *Brazilian J. Water Resour.* **29** <https://doi.org/10.1590/2318-0331.292420240033> (2014).
28. Zhang, Q., Qian, H., Xu, P., Hou, K. & Yang, F. Groundwater quality assessment using a new integrated-weight water quality index (IWQI) and driver analysis in the Jiaokou irrigation district, China. *Ecotoxicol. Environ. Saf.* **212**, 111992. <https://doi.org/10.1016/j.ecoenv.2021.111992> (2021).

29. Bian, Z. et al. A review of environment effects on nitrate accumulation in leafy vegetables grown in controlled environments. *Foods* **9**, 732. <https://doi.org/10.3390/foods9060732> (2020).
30. Shortle, J., Ollikainen, M. & Iho, A. *Water Quality and Agriculture: Economics and Policy for Nonpoint Source Water Pollution* (Springer International Publishing, 2021).
31. Drechsel, P., Marjani Zadeh, S. & Salcedo, F. P. *Water quality in agriculture: risks and risk mitigation*. Rome, Italy: FAO; Colombo, Sri Lanka: International Water Management Institute (IWMI). 192p.; Available online: <https://hdl.handle.net/10568/131888> (accessed on 13 (2024). <https://doi.org/10.4060/cc7340en> (2023).
32. Zaresefat, M., Hosseini, S. & Ahrari Roudi, M. Addressing nitrate contamination in groundwater: the importance of Spatial and Temporal Understandings and interpolation methods. *Water* **15**, 4220. <https://doi.org/10.3390/w15244220> (2023).
33. Guo, Y. F., Mi, G. H., Chen, F. J. & Zhang, F. S. Effect of  $\text{NO}_3^-$ -N supply on lateral root growth in maize plants. *J. Plant. Physiol. Mol. Biol.* **31**, 90–96 (2005).
34. Dou, C. & Sun, Y. Effect of Different Nitrogen Levels on Water and Nitrate Distribution in Aeolian Sandy Soil under Drip Irrigation. *Agronomy* **14**, 798. (2024). <https://doi.org/10.3390/agronomy14040798>
35. Jiménez-Espinosa, R., Molina-Sánchez, L., Pulido-Bosch, A. & Navarrete, F. Geostatistical study of nitrate contents in the aquifers of Campo de Dalias (SE Spain). In: (eds Soares, A., Gómez-Hernandez, J. & Froidevaux, R.) geoENVI — Geostatistics for Environmental Applications. Quantitative Geology and Geostatistics 9. Springer, Dordrecht. [https://doi.org/10.1007/978-94-017-1675-8\\_12](https://doi.org/10.1007/978-94-017-1675-8_12) (1997).
36. Li, P., Karunanidhi, D., Subramani, T. & Srinivasamoorthy, K. Sources and consequences of groundwater contamination. *Arch. Environ. Contam. Toxicol.* **80**, 1–10. <https://doi.org/10.1007/s00244-020-00805-z> (2021).
37. Ibrahim, K. O., Gomo, M. & Oke, S. A. Groundwater quality assessment of shallow aquifer hand dug wells in rural localities of Ilorin northcentral nigeria: Implications for domestic and irrigation uses. *Groundw. Sustain. Dev.* **9**, 100226. <https://doi.org/10.1016/j.gsd.2019.100226> (2019).
38. Kasem, A. M. et al. Nitrate source and transformation in groundwater under urban and agricultural arid environment in the southeastern nile delta, Egypt. *Water* **16**, 22. <https://doi.org/10.3390/w16010022> (2024).
39. Bemoussat, A. Impact de l'activité agricole sur la qualité des eaux souterraines à travers le bassin de la Tafna. Magister Thesis, University of Tlemcen, Tlemcen, Algeria, (2012).
40. Bemoussat, A., Adjim, M. & Bensaoula, F. Irrigation with treated wastewaters and the protection of Hennaya groundwater-Tlemcen, Algeria. *J. Water Land. Dev.* **43**, 19–27. <https://doi.org/10.2478/jwld-2019-0059> (2019).
41. Khouli, M. R., Haouchine, A. & Banton, O. Deterioration of the quality of groundwater in agricultural region. Case Mitidja (Algeria). *J. Fundam Appl. Sci.* **13**, 172–184. <https://doi.org/10.4314/jfas.v13i1.10> (2021).
42. Zufiurre, R., Martín-Ramos, P. & Cuchí, J. A. Nitrates in groundwater of small shallow aquifers in the Western side of Hoya de Huesca (NE Spain). *Agronomy* **10**, 22. <https://doi.org/10.3390/agronomy10010022> (2020).
43. Bourmada, A. et al. Integrated assessment of groundwater quality in algeria's Souk Ahras region: implications for sustainable and management water for drinking and irrigation purpose. *Desalination Water Treat.* **320**, 100827. <https://doi.org/10.1016/j.dwt.2024.100827> (2024).
44. Tili-Zrelli, B., Gueddari, M. & Bouhlila, R. Spatial and Temporal variations of water quality of Mateur aquifer (Northeastern Tunisia): Suitability for Irrigation and Drinking Purposes. *J. Chem.* **2408632**. <https://doi.org/10.1155/2018/2408632> (2018).
45. Bahukhandi, K. D. et al. Hydrogeochemical evaluation of groundwater for drinking and irrigation purposes in the upper Piedmont area of hardiwar, India. *ACS ES&T Water.* **3** (6), 1641–1653. <https://doi.org/10.1021/acs.estwater.2c00419> (2023).
46. Bahukhandi, K. D., Kushwaha, A., Devi, G., Goswami, L. & Bhan, U. Hydro-geochemistry of the bindal river catchment: water suitability for irrigation and drinking in the Doon Valley outer himalaya. *Int. J. Environ. Anal. Chem.* **1**–25. <https://doi.org/10.1080/03067319.2024.2436604> (2024).
47. Sathe, S. S. et al. Fluoride distribution, groundwater quality and health risk assessment for contaminated region near Krishna river (Maharashtra) India. *Environ. Nanotechnol. Monit. Manage.* **23**, 101033. <https://doi.org/10.1016/j.jenmm.2024.101033> (2025).
48. Vinuela-Martinez, J., Correa-Peralta, M., Ramirez-Anormaliza, R. & Franco Arias, O. Vera paredes, D. Geographic information systems (GISs) based on WebGIS architecture: bibliometric analysis of the current status and research trends. *Sustainability* **16** (15), 6439. <https://doi.org/10.3390/su16156439> (2024).
49. Hayane, S. M. Contribution à l'étude géologique et hydrogéologique du bassin versant de l'oued Sikkak (région de Tlemcen). Ph.D Thesis, University of Tlemcen, Tlemcen, Algeria, (1983).
50. APHA (American Public Health Association). *Standard Methods for the Examination of Water and Wastewater* 21st edn (Washington, DC, USA, 2005).
51. Deutsch, W. J. & Siegel, R. *Groundwater Geochemistry: Fundamentals and Applications To Contamination* (CRC, 2020).
52. Freeze, R. A., Cherry, J., Groundwater & Prentice-Hall Inc. : Englewood Cliffs, NJ, USA, ; Available online: (1979). <https://gw-project.org/books/groundwater/> (accessed on 08 October 2024).
53. Zhou, Y., Li, P., Xue, L., Dong, Z. & Li, D. Solute geochemistry and groundwater quality for drinking and irrigation purposes: a case study in Xinle city, North China. *Geochemistry* **80**, 125609. <https://doi.org/10.1016/j.chemer.2020.125609> (2020).
54. Hussein, E. E., Derdour, A., Zerouali, B., Almaliki, A. & Wong, Y. J. Groundwater quality assessment and irrigation water quality index prediction using machine learning algorithms. *Water* **16**, 264. <https://doi.org/10.3390/w16020264> (2024).
55. Barakat, A., El Baghdadi, M., Rais, J., Aghezzaf, B. & Slassi, M. Assessment of Spatial and seasonal water quality variation of Oum Er Rbia river (Morocco) using multivariate statistical techniques. *Int. Soil. Water Conserv. Res.* **4**, 284–292. <https://doi.org/10.1016/j.iswcr.2016.11.002> (2016).
56. Nishanthiny, S. C., Thusyanthy, M., Barathithasan, T. & Saravanan, S. Irrigation water quality based on hydro chemical analysis, jaffna, Sri Lanka. *Am. -Eurasian J. Agric. Environ. Sci.* **7**, 100–102 (2010). <http://drwjfn.ac.lk/handle/123456789/113>
57. Wilcox, L. V. *Classification and Use of Irrigation Waters*; Circular No. 969; US Department of Agriculture: Washington, DC, USA, p. 969, (1955).
58. Bahrami, M., Zarei, A. R. & Rostami, F. Temporal and Spatial assessment of groundwater contamination with nitrate by nitrate pollution index (NPI) and GIS (case study: Fasarud plain, Southern Iran). *Environ. Geochem. Health.* **42**, 3119–3130. <https://doi.org/10.1007/s10653-020-00546-x> (2020).
59. Dindaroglu, T. The use of the GIS kriging technique to determine the Spatial changes of natural radionuclide concentrations in soil and forest cover. *J. Environ. Health Sci. Eng.* **12**, 130. <https://doi.org/10.1186/s40201-014-0130-6> (2014).
60. Alexander, A. C., Ndambuki, J., Salim, R. & Manda, A. Assessment of Spatial variation of groundwater quality in a mining basin. *Sustainability* **9**, 823. <https://doi.org/10.3390/su9050823> (2017).
61. Thomas, E. O. Evaluation of groundwater quality using multivariate, parametric and non-parametric statistics, and GWQI in ibadan, Nigeria. *Water Sci.* **37** (1), 117–130. <https://doi.org/10.1080/23570008.2023.2221493> (2023).
62. Wu, J., Li, P., Wang, D., Ren, X. & Wei, M. Statistical and multivariate statistical techniques to trace the sources and affecting factors of groundwater pollution in a rapidly growing City on the Chinese loess plateau. *Hum. Ecol. Risk Assessment: Int. J.* **26** (6), 1603–1621. <https://doi.org/10.1080/10807039.2019.1594156> (2019).
63. El Mountassir, O., Bahir, M., Hakimi, S., Faraj, T. & Carreira, P. M. Assessment of groundwater quality in the Semi-Arid environment: implications of climate change. *Limnol. Rev.* **24**, 520–542. <https://doi.org/10.3390/limnolrev24040030> (2024).
64. Şener, Ş., Varol, S. & Şener, E. Evaluation of sustainable groundwater utilization using index methods (WQI and IWQI), multivariate analysis, and GIS: the case of Akşehir district (Konya/Turkey). *Environ. Sci. Pollut. Res.* **28**, 47991–48010. <https://doi.org/10.1007/s1356-021-14106-y> (2021).

65. Batarseh, M., Imreizeeq, E., Tilev, S., Al Alaween, M. & Suleiman, W. Assessment of groundwater quality for irrigation in the arid regions using irrigation water quality index (IWQI) and GIS-Zoning maps: case study from Abu Dhabi emirate, UAE. *Groundw. Sustain. Dev.* **14**, 100611. <https://doi.org/10.1016/j.gsd.2021.100611> (2021).
66. El Osta, M., Masoud, M., Alqarawy, A., Elsayed, S. & Gad, M. Groundwater suitability for drinking and irrigation using water quality indices and multivariate modeling in Makkah Al-Mukarramah province, Saudi Arabia. *Water* **14**, 483. <https://doi.org/10.3390/w14030483> (2022).
67. Richards, L. A. *Diagnosis and Improvement of Saline and Alkali Soils*. In USDA Handbook No. 60; USDA: Washington, DC, USA, (1954).
68. Jiang, Y., Wu, Y., Groves, C., Yuan, D. & Kambesis, P. Natural and anthropogenic factors affecting the groundwater quality in the Nandong karst underground river system in yunan, China. *J. Contam. Hydrol.* **109**, 49–61. <https://doi.org/10.1016/j.jconhyd.2009.08.001> (2009).
69. Jin, Z., Qin, X., Chen, L., Jin, M. & Li, F. Using dual isotopes to evaluate sources and transformations of nitrate in the West lake watershed, Eastern China. *J. Contam. Hydrol.* **177**, 64–75. <https://doi.org/10.1016/j.jconhyd.2015.02.008> (2015).
70. Singh, G., Rishi, M. S., Herojeet, R., Kaur, L. & Sharma, K. Evaluation of groundwater quality and human health risks from fluoride and nitrate in semi-arid region of Northern India. *Environ. Geochem. Health.* **42**, 1833–1862. <https://doi.org/10.1007/s10653-019-0449-6> (2020).
71. Huang, G., Sun, J., Zhang, Y., Chen, Z. & Liu, F. Impact of anthropogenic and natural processes on the evolution of groundwater chemistry in a rapidly urbanized coastal area, South China. *Sci. Total Environ.* **463**, 209–221. <https://doi.org/10.1016/j.scitotenv.2013.05.078> (2013).
72. Simsek, C. & Gunduz, O. IWQ index: a GIS-integrated technique to assess irrigation water quality. *Environ. Monit. Assess.* **128**, 277–300. <https://doi.org/10.1007/s10661-006-9312-8> (2007).
73. Laoufi, A., Boudjema, A., Guettaia, S., Derdour, A. & Almaliki, A. H. Integrated simulation of groundwater flow and nitrate transport in an alluvial aquifer using MODFLOW and MT3D: insights into pollution dynamics and management strategies. *Sustainability* **16** (23), 10777. <https://doi.org/10.3390/su162310777> (2024).
74. FAO and AWC. Guidelines for brackish water use for agricultural production in the Near East and North-Africa region. Cairo, Egypt. ; Available online: (2023). <https://openknowledge.fao.org/handle/20.500.14283/cc3234en> (accessed on 02 November 2024).
75. Centre for Coordination of Agricultural Research and Development for Southern Africa (CCARDESA). *Crop Variety Selection*. Available online: ber (2024). <https://www.ccardesa.org/crop-variety-selection>

## Acknowledgements

The authors would like to acknowledge the Deanship of Graduate Studies and Scientific Research, Taif University for funding this work.

## Author contributions

Abdessalam Laoufi, Sabrine Guettaia, Abderezak Boudjema, Abdessamed Derdour: Conceptualization, Methodology, Software, Visualization, Investigation, Writing- Original draft preparation. Abdulrahman Seraj Al-malki, Amanuel Kumsa Bojer, Khaled A. El-Nagdy, Enas Ali: Data curation, Validation, Supervision, Resources, Writing - Review & Editing, Project administration, Funding Acquisition.

## Funding

This work is funded and supported by the Deanship of Graduate Studies and Scientific Research, Taif University.

## Declarations

### Competing interests

The authors declare no competing interests.

### Additional information

**Correspondence** and requests for materials should be addressed to A.K.B.

**Reprints and permissions information** is available at [www.nature.com/reprints](https://www.nature.com/reprints).

**Publisher's note** Springer Nature remains neutral with regard to jurisdictional claims in published maps and institutional affiliations.

**Open Access** This article is licensed under a Creative Commons Attribution-NonCommercial-NoDerivatives 4.0 International License, which permits any non-commercial use, sharing, distribution and reproduction in any medium or format, as long as you give appropriate credit to the original author(s) and the source, provide a link to the Creative Commons licence, and indicate if you modified the licensed material. You do not have permission under this licence to share adapted material derived from this article or parts of it. The images or other third party material in this article are included in the article's Creative Commons licence, unless indicated otherwise in a credit line to the material. If material is not included in the article's Creative Commons licence and your intended use is not permitted by statutory regulation or exceeds the permitted use, you will need to obtain permission directly from the copyright holder. To view a copy of this licence, visit <http://creativecommons.org/licenses/by-nc-nd/4.0/>.

© The Author(s) 2025